AD-A111 108 AIR FORCE INST OF TECH WRIGHT-PATTERSON AFB OH SCHOO--ETC F/G 6/18
DESIGN AND ADAPTATION OF AN OPTICAL SYSTEM FOR SLIT LAMP DELIVE--ETC(U)
DEC 81 D J PRASKA
UNCLASSIFIED AFIT/GEO/PH/81-6 NL

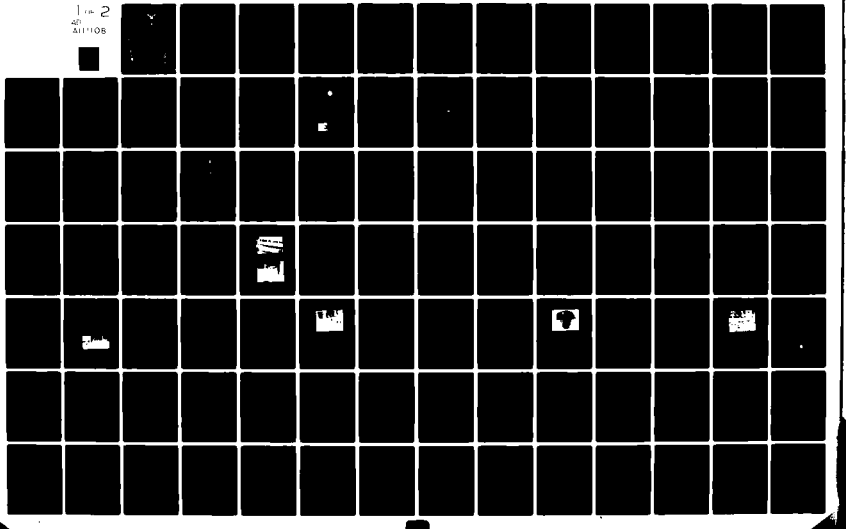

AD A111108

LEVEL

104p

DTIC FILE COPY

DTIC
ELECTE
FEB 19 1982
S
A

DEPARTMENT OF THE AIR FORCE
AIR UNIVERSITY (ATC)

AIR FORCE INSTITUTE OF TECHNOLOGY

Wright-Patterson Air Force Base, Ohio

82 02 18 030

012225

AFIT/GEO/PH/81-6

DESIGN AND ADAPTATION OF AN OPTICAL SYSTEM FOR SLIT LAMP DELIVERY OF A CO_2 LASER BEAM

THESIS

Douglas J. Praska
AFIT/GEO/PH/81-6 Capt USAF

ELECTE
FEB 19 1982
A

Approved for Public Release; Distribution Unlimited

AFIT/GEO/PH/81-6

DESIGN AND ADAPTATION OF AN OPTICAL SYSTEM FOR SLIT LAMP DELIVERY OF A CO_2 LASER BEAM

THESIS

Presented to the Faculty of the School of Engineering
of the Air Force Institute of Technology
Air University (ATC)
In Partial Fulfillment of the
Requirements for the Degree of
Master of Science

by

Douglas J. Praska, B.S.
CAPT USAF
Graduate Electro-Optics

December 1981

Accession For
DTIC
COPY
INSPECTED
2

Approved for Public Release; Distribution Unlimited

Preface

This thesis represents one of the earliest attempts to integrate a CO_2 laser to an ophthalmic slit lamp. During the project, a laser-optical system which provides ophthalmologists with limited microsurgical control was designed to direct laser radiation onto a patient's eye for the purpose of remedying ocular disorders and diseases. Someday, a similar advanced device may relieve persons with myopic disorders from having to wear prescription glasses or contact lenses. I chose this topic because of my personal fascination with how the eye and brain visualize the objects which we perceive, and because I am myopic.

I would like to express my sincere thanks to Professor Leno S. Pedrotti, my thesis advisor, who encouraged me and guided me through this research. His personal interest, rousing discussions, and helpful suggestions have been greatly appreciated.

I would also like to thank Dr. Richard H. Keates of the Ohio State University Eye Clinic for sharing his resources and expertise, and for personally testing the assembled laser-optical system by cutting corneal tissue with it. In addition, I wish to thank Ms. Angie Tornes and the rest of Dr. Keates' colleagues for their support in this project.

Thanks must also be extended to Dr. Won B. Roh, Mr. James Miskimen, and Mr. Ron Gabriel whose technical expertise provided guidance in this research project; and to Messrs

Russel Murray, David Paine, and Robert Bertke whose recommendations and craftsmanship helped me develop the laser-optical system hardware.

Finally, I wish to express my gratitude to Ms. Sharon Gabriel for her inspiration and effort in typing this thesis.

Douglas J. Praska

Table of Contents

	Page
Preface	ii
List of Figures	vi
List of Tables	vii
List of Symbols	viii
Abstract	x
I. Introduction	1
Objective and Scope	1
Background	2
Organization	10
II. Theoretical Development and Predictions	11
Beam Focusing	11
Beam Expansion	15
Apertures	17
Safety Considerations	18
Summary/Example	21
III. Spot Diameter and Rayleigh Range Dependence on Wavelength	24
IV. Experimental Equipment Design and Fabrication	29
Design Analysis	29
Design and Fabrication	32
Laser Beam Switch	34
Articulated Arm	36
Interface	38
V. System Test and Evaluation	44
Design Deficiencies	45
Optical System Transmittance	47
HeNe Laser Focusing Diagnostics	49
CO_2 Laser Focusing Diagnostics	51
Irradiation of Surgical Suture	51
Irradiation of Plastic Sheets	53
Irradiation of Corneal Tissue	54

Page

VI. Conclusions and Recommendations---------- 58

Conclusion---------- 58
Recommendations---------- 60

Bibliography---------- 62

APPENDIX A: Computer Program and Sample Results of Spot Diameter and Rayleigh Range Dependence on Wavelength, Calculations---------- 64

APPENDIX B: Detailed Prints of Laser Beam Expander, Articulated Arm, and Optical Interface---------- 69

Vita---------- 86

List of Figures

Figure		Page
1-1	A Myopic Condition	4
1-2	Radial Keratotomy, Fyodorov Method	6
1-3	Metal Scalpel Used for Radial Keratotomy	6
1-4	Flattened Cornea after Radial Keratotomy	7
1-5	Suction emplate and Blade	8
2-1	Gaussian TEM_{oo} Beam Focusing	12
2-2	Rayleigh Range	14
2-3	Galilean Beam Expander	16
2-4	Aperture of Optical Component	18
3-1	Rayleigh Range and Spot Diameter	27
4-1	Block Diagram of Proposed System	31
4-2	CO_2 Laser, Q-Switched Mode	33
4-3	Ophthalmic Slit Lamp	33
4-4	Laser Beam Switch	35
4-5	Articulated Arm	39
4-6	Optical Interface	41
4-7	Designed Laser-Optical System	43
5-1	Assembled Laser-Optical System	44
5-2	Germanium Window Assembly	46
5-3	Vertical Platform	48
5-4	Ruptured Surgical Suture	52
5-5	Pig's Eye Attached to Vertical Platform	55
5-6	Corneal Incision	56

List of Tables

Table		Page
1	Pure Metal Properties----------	37
2	Optical System Transmittances----------	49

List of Symbols

a	Radius of aperture
c	Diameter of aperture
d	Diameter of beam where it is collocated with aperture center
d_1	Diameter of beam incident on beam expander
d_2	Diameter of beam at beam expander output
d_0	Beam (spot) diameter at laser beam waist
d_{01}	Beam (spot) diameter at waist of laser beam, incident on meniscus lens
d_{02}	Beam (spot) diameter at waist of focused laser beam
f	Focal length of meniscus lens
f_1	Focal length of beam expander negative lens
f_2	Focal length of beam expander positive lens
Φ	Power of laser beam
Φ_a	Beam power transmitted through aperture
Φ_i	Beam power incident on optical component
n	Refractive index of lens

OD	Optical density value
PEL	Permissible Exposure Level
t	Exposure time of eye to laser beam
w	Radius (spot size) of beam where it is collocated with aperture center
w_{01}	Beam radius (spot size) at waist of laser beam, incident on meniscus lens
w_{02}	Beam radius (spot size) at waist of focused laser beam
z	Distance from eye to incident laser beam waist
z_1	Distance from incident beam waist to meniscus lens
z_2	Distance from meniscus lens to focused beam waist
λ	Wavelength of laser beam
θ_1	Far field half-angle beam divergence of incident beam
θ_2	Far field half-angle beam divergence of expanded beam

Abstract

A Q-switched CO_2 laser was integrated to a standard ophthalmic slit lamp with the aid of an articulated arm. The laser-optical system, including the articulated arm, was adapted to a Nikon slit lamp to provide flexible control of high power 10.6 μm radiation for use in surgical cutting of the cornea. The articulated arm, consisting of seven optical elbows and seven copper mirrors, transmitted the CO_2 radiation from the laser to a 5X beam expander and a F/1 zinc selenide focusing lens attached to the slit lamp.

Experimental results indicate that the integrated system can deliver 22 μm spots of focused radiation on target with a corresponding Rayleigh range of approximately 36 μm. To demonstrate precise beam control, 9-0 Ethicon suture was ruptured with as little as 2.4 mJ of energy. Clear plastic sheets were cut to give an indication of what to expect in a corneal incision. Finally, hog corneas were incised by an ophthalmologist.

The experimental work was complemented by a parametric study relating focused spot diameter, Rayleigh range, and laser wavelength for a series of wavelengths extending from 0.249 to 10.6 μm. The results of the parametric plots may be used as an aid when selecting optimal laser parameters for given applications in ocular surgery.

DESIGN AND ADAPTATION OF AN OPTICAL SYSTEM FOR SLIT LAMP DELIVERY OF A CO_2 LASER BEAM

I. Introduction

The laser is evolving into a significant tool for medical science. Ophthalmology, in particular, has benefitted immensely with the laser's increasing role in ocular surgery. In ophthalmic therapy, the laser has two main functions: it can substitute for a scalpel, or it can be used for intraocular scar formation (Ref 1:243). Since the laser's introduction to medical science, dedicated research has explored and exploited its efficacies for the improvement of human health. This thesis is but one step in a comprehensive research program contributing to that cause.

Objective and Scope

The thesis project is founded on two interrelated goals. The first goal is to design and fabricate a controllable, high precision, laser-optical system which can cut micro-incisions within corneal tissue, and function as a "laser scalpel" in ocular surgery, particularly radial keratotomy. The system will contain principally an existing CO_2 laser and a standard ophthalmic slit lamp optically connected together by an articulated arm. Furthermore, it will be tested and evaluated on its ability to satisfy the cutting and man-machine interface

requirements for corneal surgery. The second goal is to perform comprehensive spot diameter and Rayleigh range calculations which can help ophthalmologists in selecting optimum laser parameters for surgical procedures. These calculations will apply directly to the lasers used most frequently in ocular surgery (CO_2, Nd^{3+}:YAG, ruby and argon) and a potential surgical excimer laser (KrF^*). The calculations will also cover a limited range of spot diameters (10 μm to 40 μm).

Background

The application of lasers in medicine is not a relatively new topic. Argon, ruby, CO_2, and Nd^{3+}:YAG lasers have been employed in ocular surgery to treat an assortment of disorders and diseases for at least ten years. The argon laser is a popular photocoagulator among ophthalmologists. It is used to treat retinal diseases and offers a solution to a certain type of diabetic retinopathy (Ref 2:1518). The argon laser has also been found effective in remedying angle-closure glaucoma (Refs 3 and 4) and open angle glaucoma (Ref 5). The first laser photocoagulators were ruby lasers; they replaced the xenon arc photocoagulators of the past. Since the ruby laser exhibits certain limitations, its role is now mainly restricted to correcting retinal tears and post-retinal detachments (Ref 6). Nd^{3+}:YAG lasers are currently being introduced in ophthalmology largely on an experimental basis. In 1971 L'Esperance tested a frequency doubled

Nd^{3+}:YAG laser's efficacy to serve as a photocoagulator. A non-linear barium sodium niobate crystal converted the near infrared radiation (1.064 μm) to green light (0.532 μm). L'Esperance found this arrangement to be a promising tool in the photocoagulation of ophthalmic vascular and chorioretinal disease (Ref 7).

Recent experiments conducted with the Nd^{3+}:YAG laser indicate that it is capable of opening the opacified posterior capsule in a pseudophakic eye (Ref 8). Medical science is also studying the application of the CO_2 laser to ocular surgery. The special significance of this laser is that all ocular tissues are opaque to its radiation (Ref 9:297). Beckman and his associates have used the CO_2 laser to perform trabeculectomy-like filtering procedures for various forms of glaucoma. In addition, they have treated both lid lesions and paraocular skin lesions (Ref 10).

The CO_2 laser exhibits potential in other procedures too. Landers and his colleagues have suggested that the CO_2 laser could be used as an instrument for precision cutting of corneal buttons in keratoplasty (Ref 1:231); Karlin and his colleagues commented that it may be used to dissolve cataracts (Ref 9:297). Another possible CO_2 laser application, proposed by the ophthalmology community and to which this thesis is dedicated, is in the reduction or cure of myopia by radial keratotomy.

To acquire an understanding of the CO_2 laser's role in radial keratotomy, it is helpful to consider how radial ketatotomy can alter the myopic state.

Myopia, or nearsigntedness, is a condition of the eye in which distant objects, brought into focus by the cornea and lens, fall short of being imaged on the retina, and therefore appear blurred. The power of the corneal-lens system, as configured, is too large for the axial length of the eye, as shown in Figure 1-1.

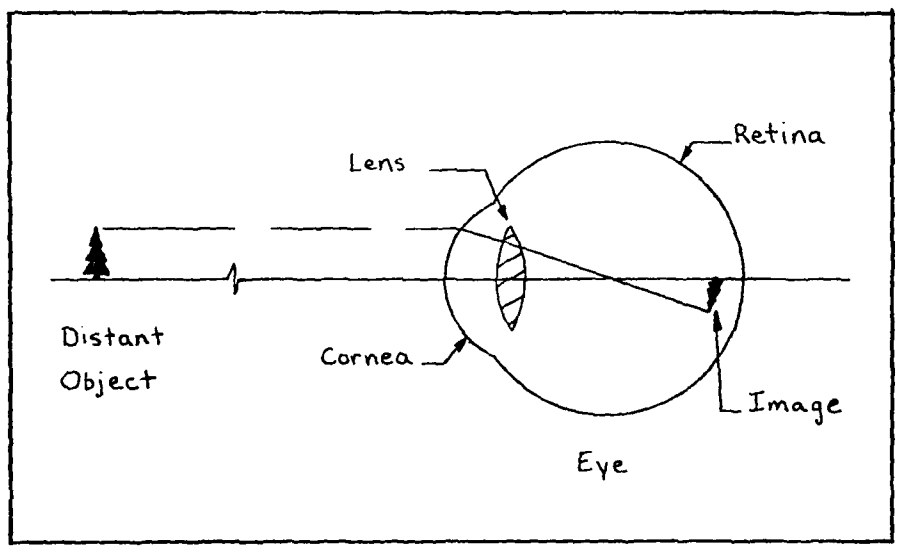

Figure 1-1. A Myopic Condition

Myopia can occur for a number of reasons: the cornea may increase in curvature which will cause incoming light rays to refract greater than normal, the eye may elongate though its power remains normal, or it may result from abnormal refractivity of the eye's optical media. To date, the majority of nearsighted cases have been corrected with

prescription spectacles or contact lenses. Some myopic conditions have been remedied through orthokeratology -- a mechanical technique which reduces corneal curvature as the patient wears a series of hard contact lenses.

Another form of correction that decreases myopia (on the order of a few diopters or to the point of near perfect vision) is an experimental procedure known as radial keratotomy. Fyodorov and Durnev report that, in this operation, the ophthalmologist begins by making a series of careful calculations on the corneal shape of the patient's eye. After placing several anesthetizing drops onto the patient's eye, a thin rigid disc is pressed onto the cornea. Pressure exerted on the disc produces sixteen equally spaced indentations on the cornea, which radiate outward from the perimeter of the pupil to the limbus, as illustrated in Figure 1-2. With these indentations as a guide, the ophthalmologist makes sixteen tiny incisions, using a special metal scalpel as shown in Figure 1-3. The insert in Figure 1-3 is a 10X magnification of the scalpel's blade.

The depths of Fyodorov's cuts approach three-fourths of the thickness of the cornea (approximately 0.455 mm) and are controlled by direct microscopic vision. This technique is believed to work because the dissection of the circular collagen fibers sharply weakens the mechanical stability of the cornea. Intraocular pressure then causes the incised portion of the cornea to bulge slightly outward, which in

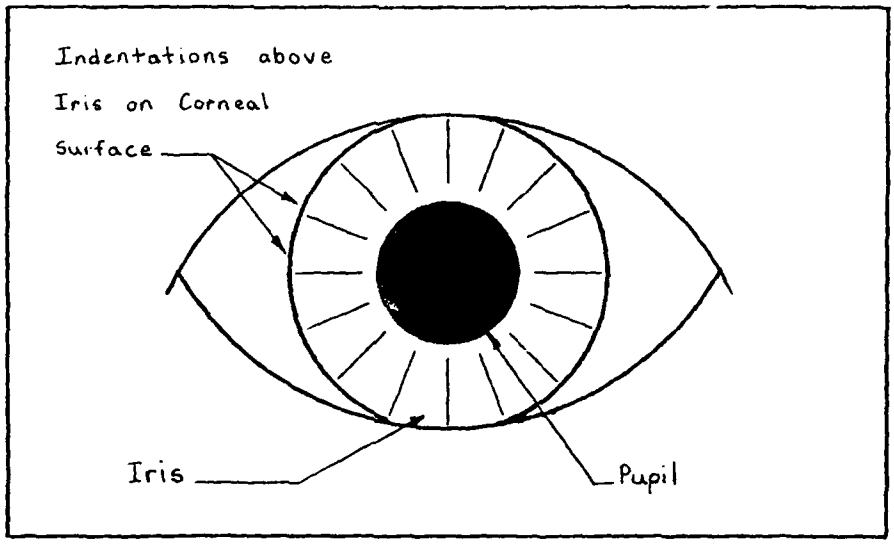

Figure 1-2. Radial Keratotomy, Fyodorov Method

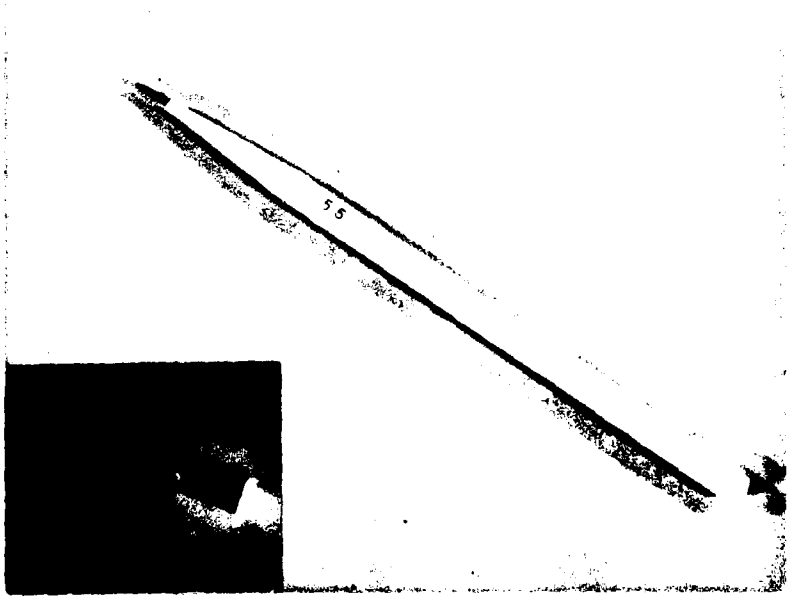

Figure 1-3 Metal Scalpel Used for Radial Keratotomy. (Courtesy of Dr. R.H. Keates, Ohio State University Eye Clinic.

turn flattens the cornea and lessens the refraction of incoming light (Ref 12). Figure 1-4 is an exaggerated sketch depicting a flattened cornea.

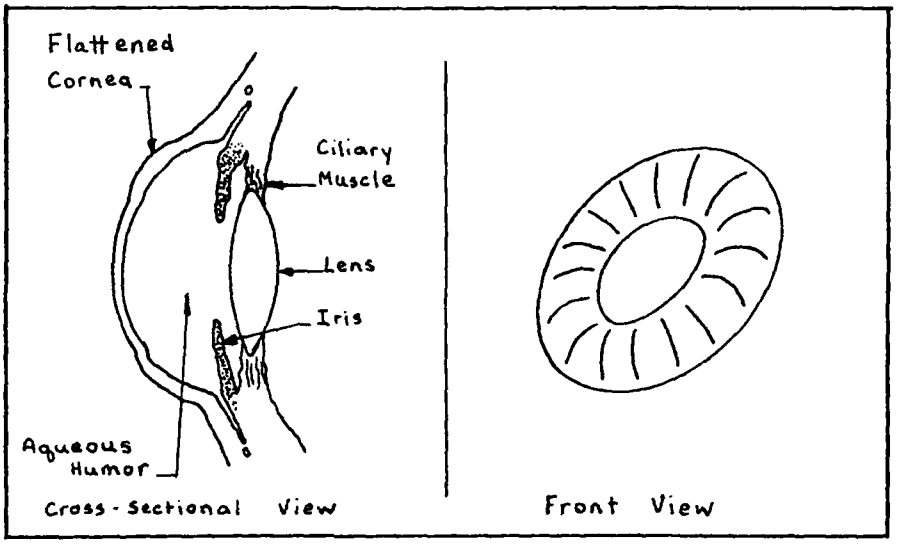

Figure 1-4. Flattened Cornea After Radial Keratotomy

Success of this operation is dependent upon precise depths and lengths of the incisions. A mathematical model, developed by Schachar and his colleagues, predicts the depths and lengths of the required incisions, and is consistent with clinical findings (Ref 12:195-220).

To ensure accurate cutting, a few ophthalmologists employ scalpels with depth adjustment controls and a special gauge to measure uniformity and depth. Kramer and his associates have performed radial keratotomies with a cutting template which is affixed to the cornea by suction. The template is transparent, plastic, and contains eight equal-length radial slots. It is meniscus-convex in shape to

allow for deeper incisions at the periphery where the cornea is thicker. A specially designed scalpel fits onto the template to make the incisions. The shape of the cornea does not change as incisions are made; however, when the suction template is removed, the cornea relaxes (Ref 13). Figure 1-5 is a representation of the integrated template and surgical blade.

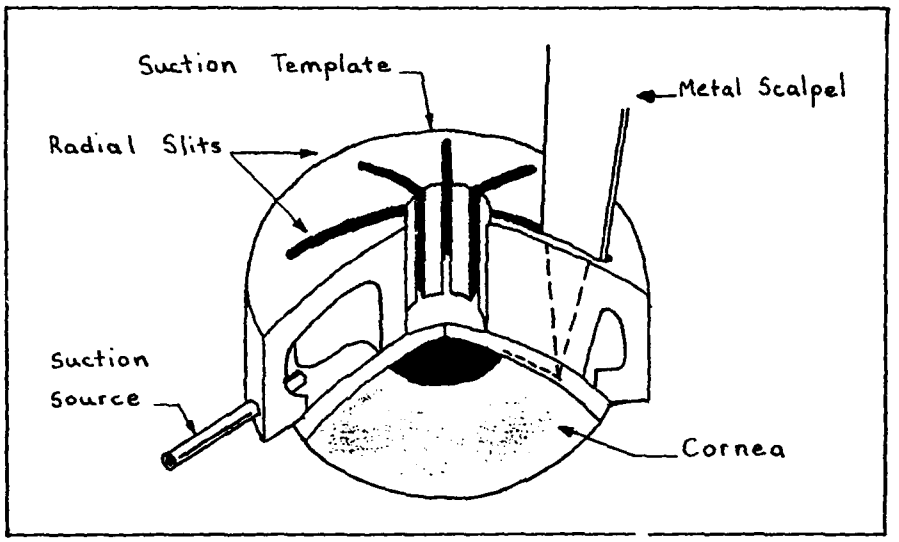

Figure 1-5. Suction Template and Blade

Recently, interest has been generated for the use of CO_2 lasers in performing radial keratotomies. First, a laser scalpel could ensure more precise incision depths and lengths, since exact pressures and frictional drag associated with conventional metal scalpels would be eliminated. Second, no visual obstructions would hinder the ophthalmologist's field of view, and third, a laser beam sterilizes the neighboring tissue around an incision as it cuts (Ref 14). With

a laser, an ophthalmologist could match the calculated incision parameters precisely by selecting the correct beam power, cutting speed, spot diameter, and number of passes.

The CO_2 laser is ideally suited for radial keratotomy. Of the four popular previously named lasers employed in medicine, only CO_2 energy (10.6 μm) is completely absorbed by the cornea. The radiation emitted from the other laser sources pass almost unnoticeably through the cornea and are absorbed mainly by the retina, choroid, and sclera (Refs 15 and 16).

As a first step toward performing corneal surgery with a CO_2 laser, the Air Force Institute of Technology Physics Department, with assistance from the Ohio State University Eye Clinic, sponsored a thesis project on the design and construction of a CO_2 laser-optical system which would exhibit precise control of power output, beam divergence and spot size (Ref 17). The system was tested by cutting thermal copying paper, plastic sheets, surgical sutures, and finally, animal and human corneas. The laser was evaluated in three different modes of operation: continuous wave, externally chopped, and Q-switched. Experimental results showed that a CO_2 laser-optical system can make corneal incisions with a controllable penetration depth greater than or equal to 50 μm and a width as narrow as 50 μm. Of the three modes, the Q-switched mode was considered optimum since it created

the least charring in the corneal tissue. Having demonstrated accurate beam control, it was concluded that the CO_2 laser could supplement or replace metal scalpels in some surgical procedures of the cornea. Finally, it was recommended that the existing CO_2 laser be integrated with a standard slit lamp to provide a safe and useful tool for corneal surgery. This thesis project was founded on that recommendation.

Organization

Chapter II contains the theory which supports the design of the CO_2 laser-optical system constructed in this thesis. It addressed the focusing of gaussian laser beams, the effects rendered on them by apertures, and the safety precautions which should be considered when working with them. Chapter III discusses the relationship between spot diameter and corresponding Rayleigh range for various wavelengths. Chapter IV describes the experimental design and fabrication of the CO_2 laser-optical system. Chapter V contains the test and evaluation results, and lastly, Chapter VI presents the conclusions and recommendations.

II. Theoretical Development and Predictions

Corneal tissue is an excellent absorber of infrared radiation. Therefore, when high power CO_2 energy is concentrated onto the cornea, it is instantaneously converted into intense heat, which in turn vaporizes the tissue and creates a narrow cut or incision. Through careful monitoring and control, a CO_2 laser beam can be used to burn through ocular tissue, creating clean incisions of controllable width and depth.

When microsurgery such as radial keratotomy is performed on the eye, whether it is done using a special metal scalpel or a "laser scalpel," serious consideration must be given to the width and depth of the incisions. Ideally, the "scalpel" should be as narrow as possible and penetrate as deep as the ophthalmologist requires. These two parameters, in regard to a laser scalpel, are directly proportional to the spot diameter and Rayleigh range, respectively, of the focused laser beam. The topics covered in this chapter address those parameters and a few others for tailored laser beams. These topics include beam focusing, beam expansion, apertures, and safety considerations. The theory is based on gaussian TEM_{oo} beam propagation.

Beam Focusing

Generally speaking, CO_2 laser beams emitted from their sources are too large for making acceptable incisions within

the cornea; therefore, focusing is required to reduce their spot diameters. Consider a gaussian TEM_{oo} laser beam incident upon and focused by a converging lens as shown in Figure 2-1.

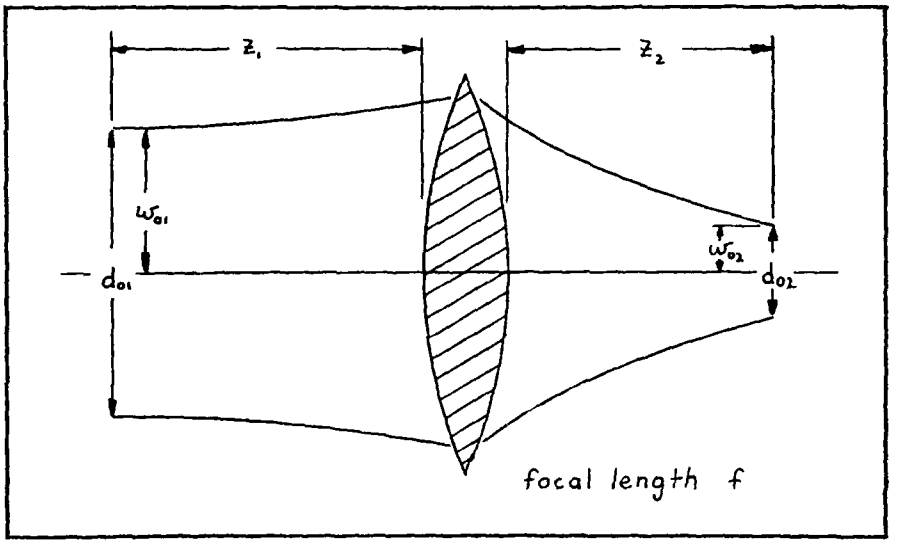

Figure 2-1. Gaussian TEM_{oo} Beam Focusing

The incident beam has a spot size (w_{01}) located, at its waist, a distance z_1 in front of the lens having a focal length f. The focused beam has a spot size (w_{02}) positioned, at its waist, a distance z_2 behind the lens. The focused beam spot size can be determined by applying the following equation:

$$\frac{1}{w_{02}^2} = \frac{1}{w_{01}^2}\left(1 - \frac{z_1}{f}\right)^2 + \frac{1}{f^2}\left(\frac{\pi w_{01}}{\lambda}\right)^2 \qquad (1)$$

where λ is the wavelength of the laser beam (Ref 18:31).

If it is assumed that w_{01} is much greater than w_{02}, then Eq (1) can be simplified to

$$w_{02} = f\left(\frac{\lambda}{\pi w_{01}}\right) \tag{2}$$

By inspection, the term in parentheses is seen to be identical to the far field half-angle divergence (θ) for a gaussian beam (Ref 19:34). Moreover, Eq (2) can be rewritten in terms of the spot diameters for the incident and focused laser beams, at their respective waists, as

$$d_{02} = 1.273\,\frac{f\lambda}{d_{01}} \tag{3}$$

where d_{01} equals $2w_{01}$ and d_{02} equals $2w_{02}$.

One can see from Eq (3) that the focused beam diameter is directly proportional to the wavelength and focal length, and inversely proportional to the diameter of the incident beam.

Contrary to what is predicted in geometrical optics, the waist of a focused gaussian laser beam may not be centered in the focal plane of a converging lens. Rather, using gaussian optics, it is found, in general, that the waist will be formed slightly to one side of the focal plane, as shown in Eq (4) (Ref 18:31).

$$z_2 = f + \frac{f^2(z_1-f)}{(z_1-f)^2 + \left(\frac{\pi w_{01}^2}{\lambda}\right)^2} \tag{4}$$

Note that the position of the waist is principally dependent upon the focal length of the lens. However, it is also dependent upon the incident beam's wavelength, waist location, and spot size at the waist. If z_1 is equal to or much greater than f, then z_2 will equal f and the focused beam will form in the focal plane of the converging lens.

Rayleigh range is defined as the distance from a beam's waist to the on-axis point where its cross sectional area has doubled in size. The beam is considered to be "collimated" within a Rayleigh range of the beam. These parameters are illustrated in Figure 2-2.

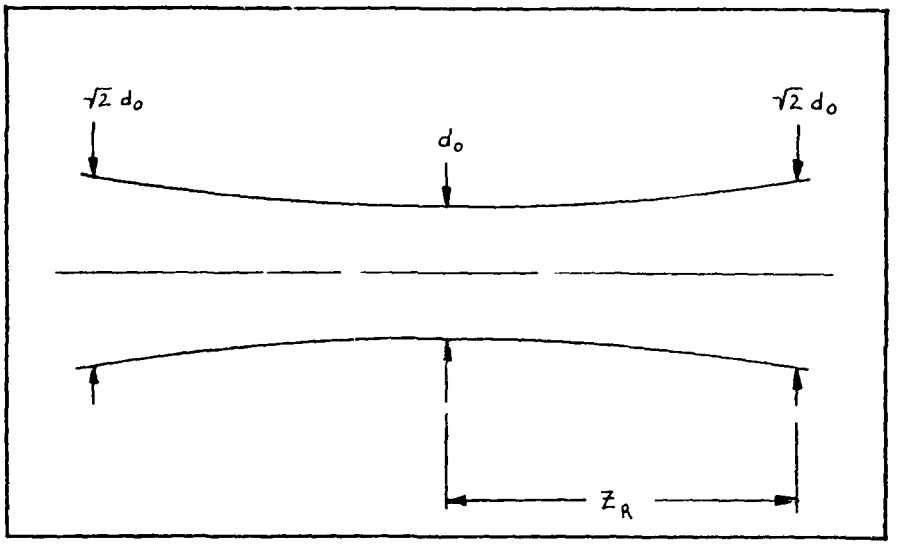

Figure 2-2. Rayleigh Range

Within this span, the irradiance of the beam has sufficient magnitude to vaporize corneal tissue -- producing an incision. Rayleigh range is directly proportional to the square of the spot size at the beam's waist and inversely

proportional to its wavelength. It can be calculated using Eq (5) (Ref 20:312).

$$z_R = \frac{\pi w_0^2}{\lambda} \tag{5}$$

In terms of the spot diameter, the Rayleigh range can be rewritten as

$$z_R = \frac{\pi d_0^2}{4\lambda} \tag{6}$$

Beam Expansion

Being able to produce an acceptable, microscopic spot diameter -- in turn, incision width -- is a key factor in determining whether the CO_2 laser can be applied to corneal surgery. Referring back to Eq (3), it is evident that the focused beam diameter (d_{02}) will decrease as the incident beam diameter (d_{01}) increases. Therefore, expanding the incident beam before it strikes the converging lens should render the focused beam even smaller, provided that the lens is greater than the expanded beam.

Consider a Galilean beam expander, composed of two lenses, illustrated in Figure 2-3. The front lens has a negative focal length (f_1) and the back lens has a positive focal length (f_2). The two lenses are afocal; i.e., they are separated by a distance equal to the sum of their focal lengths. When combined, they function as a simple telescope.

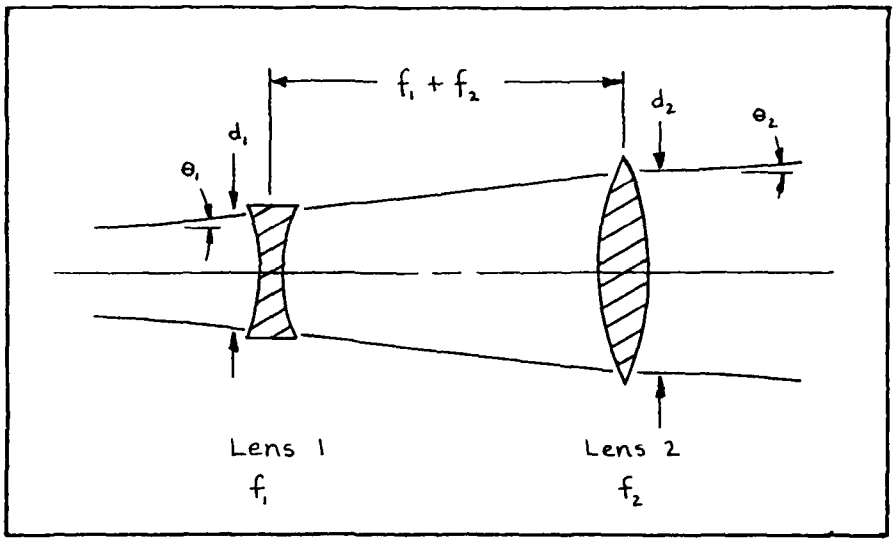

Figure 2-3. Galilean Beam Expander

Let the input beam diameter and far field half-angle beam divergence, at the front surface of the first lens, be denoted as d_1 and θ_1, respectively. Similarly, let the output beam diameter and far field half-angle divergence, at the back surface of the second lens, be designated as d_2 and θ_2. Using ray matrix techniques, applied to TEM_{oo} gaussian beams, it can be shown that the input and output beams are related by

$$d_2 = \left|\frac{f_2}{f_1}\right| d_1 \tag{7}$$

and

$$\theta_2 = \left|\frac{f_1}{f_2}\right| \theta_1 \tag{8}$$

These equations indicate that the incident beam is enlarged by a factor equal to the quotient of the focal lengths, and the beam divergence is reduced by a factor equal to the inverse of that same quotient. Note that these results fortify the assumptions used to reduce Eq (1) to Eq (2).

Apertures

Occasionally, when gaussian laser beams are to be shaped, they may be passed through lenses or reflected from mirrors. When this occurs, it is very important to know the dimensions of the aperture of the beam shaping optical component, relative to the diameter of the laser beam. By proper design of the optical component, all of the beam's energy will propagate forward, and negligible diffraction effects will be introduced by the beam shaping optical component. The ratio of the power (Φ_a) transmitted through or reflected from a circular aperture of radius a, to the power (Φ_i) incident upon the optical component, as shown in Figure 2-4, is given by

$$\frac{\Phi_a}{\Phi_i} = 1 - \exp\left\{\frac{-2a^2}{w^2}\right\} \tag{9}$$

where w is the spot size of the beam at the point where it is collocated with the aperture (Ref 20:312). Note that Eq (9) does not take into account the reflectance or transmittance properties associated with the material of the beam shaping optical component. In terms of beam diameter (d)

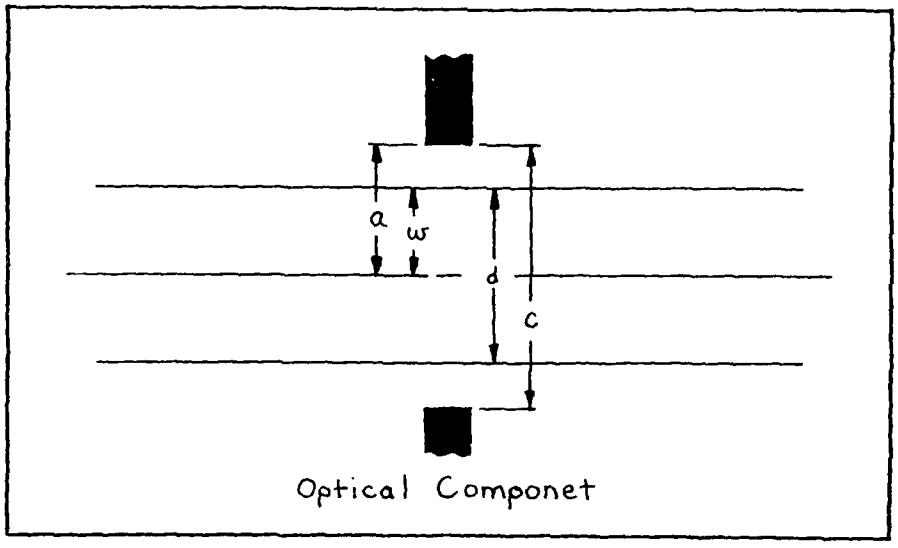

Figure 2-4. Aperture of Optical Component

and aperture diameter (c), Eq (9) can be rewritten as

$$\frac{\Phi_a}{\Phi_i} = 1 - \exp\left\{\frac{-2c^2}{d^2}\right\} \qquad (10)$$

As a rule of thumb, Siegman states that an aperture of diameter 1.5 times the gaussian beam diameter will pass approximately 99 percent of the beam power and that diffraction effects will be negligible.

Safety Considerations

Performing operations with lasers requires practice of special precautions to avoid unintentional beam exposure to the eye. Direct ocular exposure to the laser beam may damage the eye. The damage incurred is a function of the

incident laser beam power (Φ), distance from the beam waist to the eye (z), spot size at the waist (w_0), wavelength (λ), and exposure time (t). The U.S. Air Force has conducted extensive research investigating permissible laser exposure levels (PEL) for the human eye (Refs 21 and 22). The PEL, an irradiance, is related to the incident beam power by

$$PEL = \frac{\Phi}{\pi b^2} \tag{11}$$

where b is the spot size corresponding to the e^{-1} irradiance value of the incident gaussian beam on the corneal surface. The worst case exposure condition, for a laser beam damaging the retina, occurs when the collimated beam fills the pupil and exhibits a waist at the eye's near point. This is due to the focusing properties of the cornea and the lens. The spot size for the incident laser beam is defined as

$$b = \frac{w_0}{2^{\frac{1}{2}}} \left[1 + \left(\frac{\lambda z}{\pi w_0^2}\right)^2\right]^{\frac{1}{2}} \tag{12}$$

Substituting Eq (12) into Eq (11), setting $w_0 = d_0/2$ where d_0 is the spot diameter at the waist, and solving for the power yields

$$\Phi = \frac{\pi (PEL) d_0^2}{8} \left[1 + \left(\frac{4\lambda z}{\pi d_0^2}\right)^2\right] \tag{13}$$

This equation may be interpreted as the maximum permissible power at the waist of a laser beam, incident upon and located a distance z from the eye, which will not cause damage to the eye. The PEL is dependent upon spectral range, exposure time, and waveform of the laser beam. A PEL of 1.8×10^{-3} $t^{-\frac{1}{4}}$ watts/cm^2 is valid for a spectral range stretching from 0.4 μm to 1.4 μm (except for 1.06 μm), an exposure time extending from 19 μs to 10 s, and a continuous wave output. Incorporating this PEL value into Eq (13) produces

$$\Phi = \frac{9\pi d_0}{40{,}000\ t^{\frac{1}{4}}} \left[1 + \left(\frac{4\lambda z}{\pi d_0^2}\right)^2\right] \tag{14}$$

Generally, the true power (Φ_t) of an incident laser beam is greater than Φ. If so, a protective shield covering the eye or a neutral density filter inserted within the optical system is required. The degree of protection is given in optical density (O.D.) which is defined by

$$\text{O.D.} = \log_{10} \left\{\frac{\Phi_t}{\Phi}\right\} \tag{15}$$

Combining Eqs (14) and (15) yields the following expression for computing the minimum optical density value of a neutral density filter which ensures adequate ocular protection from the incident laser beam.

$$\text{O.D.} = \log_{10} \left\{\frac{40{,}000\ \Phi_t t^{\frac{1}{4}}}{9\pi d_0^2} \left[1 + \left(\frac{4\ z}{\pi d_0^2}\right)^2\right]^{-1}\right\} \tag{16}$$

This equation will provide valid accurate optical density values only when the incident laser beam waist is located at or beyond the near point of the eye, again due to the focusing of the cornea and the lens. If the visible laser beam is focused between the eye and its near point, then the worst case condition must be considered and z should be set equal to 7.0 cm, the approximate distance from the cornea to the near point of a normal young adult eye.

Summary/Example

This chapter has thus far provided the background theory required to develop a laser scalpel for corneal surgery. In concluding this chapter, a series of calculations is performed using the derived formulae. The numerical values used in these examples match closely to those which characterize the designed laser-optical system.

Take the spot diameter and far field half-angle beam divergence for the CO_2 laser beam (10.6 μm) at the input of the 5X Galilean beam expander to be 7 mm and 1.1 mrad, respectively. If the negative lens of the beam expander has a focal length of -2 cm and the positive lens has a focal length of 10 cm, then the output spot diameter and far field beam divergence from Eqs (7) and (8) are

$$d_2 = \left| \frac{f_2}{f_1} \right| d_1 = 5.5 \text{ cm}$$

and

$$\theta_2 = \left| \frac{f_1}{f_2} \right| \theta_1 = 0.22 \text{ mrad}$$

If this expanded and nearly collimated gaussian laser beam is now directed upon a converging lens with a focal length of 3.81 cm, then employing Eq (3), the focused beam would exhibit a spot diameter of

$$d_{02} = 1.273 \frac{f\lambda}{d_{01}} = 14.7 \text{ } \mu\text{m}$$

at its waist. Suppose the incident beam waist lies at a distance from the lens much greater than the focal length of the lens, then the location of the focused beam waist according to Eq (4) is

$$z_2 = f = 3.81 \text{ cm}$$

The Rayleigh range of the focused beam can now be determined from Eq (6) using the spot diameter d_{02} calculated above.

$$z_R = \frac{\pi d_{02}^2}{4\lambda} = 16.0 \text{ } \mu\text{m}$$

The last three calculated figures imply that the given laser-optical system could theoretically produce incisions 3.81 cm

from the converging lens, which are approximately 14.7 μm wide and 16.0 μm deep.

Now suppose an articulated arm is used to route the CO_2 laser energy into the beam expander from the laser source. Following Siegman's rule of thumb, the minimum internal diameter of the arm required to pass the laser energy without transmission or diffraction losses would be

$$c = 1.5d = 1.05 \text{ cm}$$

For a final calculation, consider laser safety requirements. Let a HeNe laser beam (0.6328 μm), colineated with a CO_2 laser beam, be used for targeting the CO_2 laser energy onto a patient's cornea. If the HeNe radiation focused on the cornea exhibits a working power of 0.02 mWatts, a spot diameter of 3.5 μm, and an exposure time of 10 s, then the minimum optical density, for a neutral density filter, required to protect the patient's and ophthalmologist's eyes would have to be, employing Eq (16)

$$\text{O.D.} = \log_{10} \left\{ \frac{40{,}000\ \Phi_t t^{\frac{1}{4}}}{9\pi d_0^{\,2}} \left[1 + \left(\frac{4\lambda z}{\pi d_0^{\,2}} \right)^2 \right]^{-1} \right\} = 2.3$$

III. Spot Diameter and Rayleigh Range Dependence on Wavelength

Before an ocular disorder or disease can be remedied using a laser-optical device on a microsurgery level, the ophthalmologist must consider four important laser parameters: wavelength, beam power, spot diameter, and Rayleigh range. Optimal values for these variables should be chosen to maximize the success of the patient's postoperative recovery. During this research period, comprehensive calculations were performed to help ophthalmologists select optimal spot diameter and Rayleigh range values. These parameters are important since they directly affect the incision width and depth. Power is not addressed in this chapter, and wavelength is chosen only to represent the ranges available with lasers in current use.

The two pertinent equations from which the calculations are based were derived in Chapter II. These equations are

$$d_{02} = 1.273 \lambda \frac{f}{d_{01}} \tag{3}$$

and

$$z_R = \frac{\pi d_{02}^2}{4\lambda} \tag{6}$$

As noted in Chapter II, the spot diameter and Rayleigh range for a focused laser beam are wavelength dependent and are not independent of one another. The focused spot diameter is directly proportional to, and the Rayleigh range is inversely proportional to, the laser beam wavelength. In addition, the Rayleigh range is proportional to the square of the focused spot diameter.

The calculations incorporate five different wavelengths so that spot diameter and Rayleigh range values for five different lasers can be compared. Four of the wavelengths correspond to lasers already used in medicine; they include: CO_2 (10.6 μm), Nd^{3+}:YAG (1.06 μm), Ruby (0.694 μm), and Argon (0.488 μm). Krypton fluoride (0.249 μm) was chosen as the fifth laser to compare its theoretical ultraviolet capabilities to those of infrared and visible lasers.

If laser-optical devices are to be appreciated and accepted in ocular surgery (possibly to replace metal scalpels), then they must meet certain criteria. In particular, those instruments which are designed to function as laser scalpels should be capable of producing narrow incisions which are comparable in width to those obtained using the finest metal scalpels. With this point in mind, the computation process begins by generating a limited range of f/d_{01} values for the focusing lens. This quotient represents the focal length of the converging lens to the incident laser beam spot diameter on the lens. Practical values for

the ratio f/d_{01} were chosen to range from one to twenty in increments of one-eighth. Focused spot diameters were calculated using Eq (3) and were truncated at a maximum value of 42 microns. Corresponding values of Rayleigh range were then calculated using Eq (6). Figure 3-1 represents the final results for each of the five trial wavelengths. The computer program is provided in Appendix A for any further analysis.

In Figure 3-1, the CO_2 laser line is far removed from the others; this is due to its long infrared wavelength. As the CO_2 laser beam is focused to smaller spot diameters, the Rayleigh range is seen to decrease at a more rapid rate. Eventually, the Rayleigh range approaches values having the same order of magnitude as the spot diameter. This is a serious problem which inhibits the cutting of deep incisions. Incisions can be made deeper by retracing, but not without unacceptable widening of the tissue. Another infrared laser, the Nd^{3+}:YAG, can achieve longer Rayleigh range values than the CO_2 laser for any given spot diameter. This occurence is due to the fact that the Nd^{3+}:YAG laser wavelength is one-tenth the size of the CO_2 laser's. The visible lasers, Ruby and Argon, share very similar focusing properties which are better than those of the Nd^{3+}:YAG and CO_2 lasers. Lastly, the Krypton Fluoride laser, of the five lasers considered, yields the longest Rayleigh range for any given spot diameter.

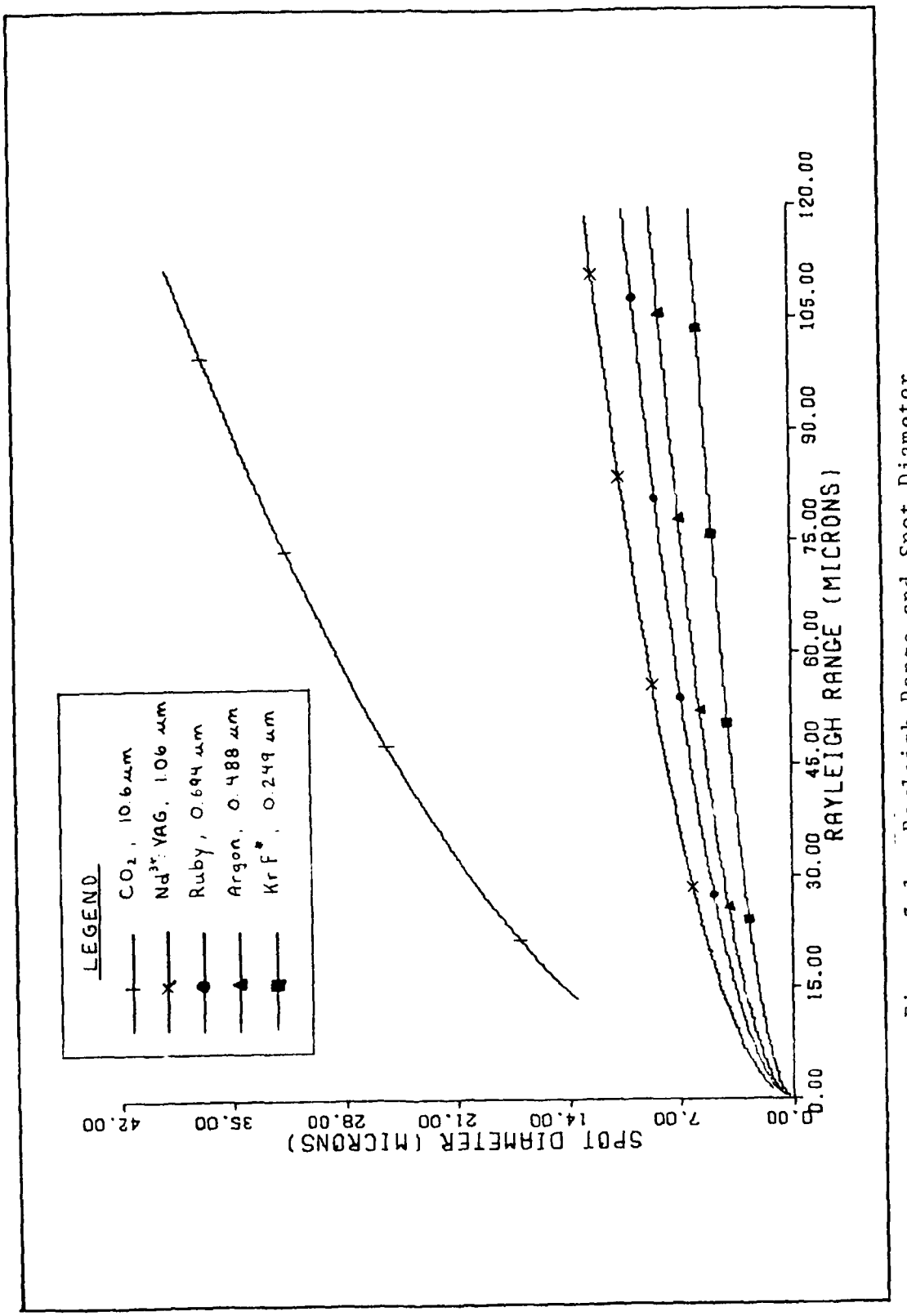

Figure 3-1. Rayleigh Range and Spot Diameter

In summary, the tradeoffs in selecting a laser or adjusting its optical system for ocular surgery are easily readable in Figure 3-1. Spot diameters of ocular laser instruments, at any wavelength, can be manipulated by varying the optical components within. However, for any given optical configuration, lasers with shorter wavelengths can be focused to smaller spot diameters (consequently, smaller incision widths). In addition, shorter wavelength lasers also provide longer Rayleigh ranges (in turn, deeper incisions of uniform width) for any given spot diameter. Therefore, ultraviolet lasers, such as the KrF* laser which can deliver small spot diameters with long Rayleigh ranges, may be ideally suited for ocular surgery since much of the ocular media absorbs ultraviolet radiation in the 0.25 μm range. However, the biological effect of intense ultraviolet radiation on the corneal tissue, adjacent to and immediately beneath the incision, must yet be determined.

IV. Experimental Equipment Design and Fabrication

Design Analysis

Utilizing the theory derived in Chapter II, an optical system was constructed using commercial and custom-built components. The intent was to design and fabricate a laser scalpel suitable for corneal surgery, whereby the working system would be readily adaptable to an ophthalmologist's needs and easily controlled with microscopic precision.

Before this thesis was started, it was concluded that the best interface between the CO_2 laser system and the ophthalmologist would be a device which is very familiar to ophthalmologists -- the slit lamp. A reconfigured slit lamp, similar to the commercially made 900 Argon Laser Photocoagulator, would be ideal (Ref 23). Such a device would offer an ophthalmologist excellent viewing while cutting ocular tissue and precise microscopic control of the laser beam. Thus, it was decided to feed the CO_2 laser beam into a slit lamp.

The major challenge was to develop an optical component which would channel the laser beam from its source into a slit lamp, all the while retaining a full three degrees of freedom. Flexibility is required because incisions cannot be made with a rigid optical delivery arm. Fiber optic cables would have been the ideal medium; however, technology has yet

to develop a fiber optic cable which is capable of transmitting CO_2 radiation at 10.6 μm with low attentuation (Ref 24). An articulated arm would then have to suffice and be incorporated.

It was also reasoned that, since a CO_2 laser beam is infrared and invisible, a targeting capability would have to be implemented within the system. Without this capability, an ophthalmologist could not accurately focus the CO_2 laser beam onto a patient's eye. Targeting would be required only at the onset of an incision, since an ophthalmologist could track and guide the CO_2 laser beam as it cut corneal tissue by observing the incision. A severely attenuated low power HeNe laser, emitting radiation at a wavelength of 0.6328 μm, with its red beam coaxially merged with the CO_2 laser beam in the system, would be sufficient for targeting. This technique, with the aid of a switching mechanism, has already been successfully utilized in a few infrared laser systems.

Finally, it was conceived that the focusing optical elements, identified in Chapter II, would have to be housed in a unit at the slit lamp. This optical interface would then accept the laser radiation and focus it onto the patient's eye. A block diagram of the proposed system is depicted in Figure 4-1.

At the start of any design phase, the designer must thoroughly understand what the input to the system will be, and what is expected at its output. The heart of this system is the CO_2 laser, which emits infrared radiation at a wavelength

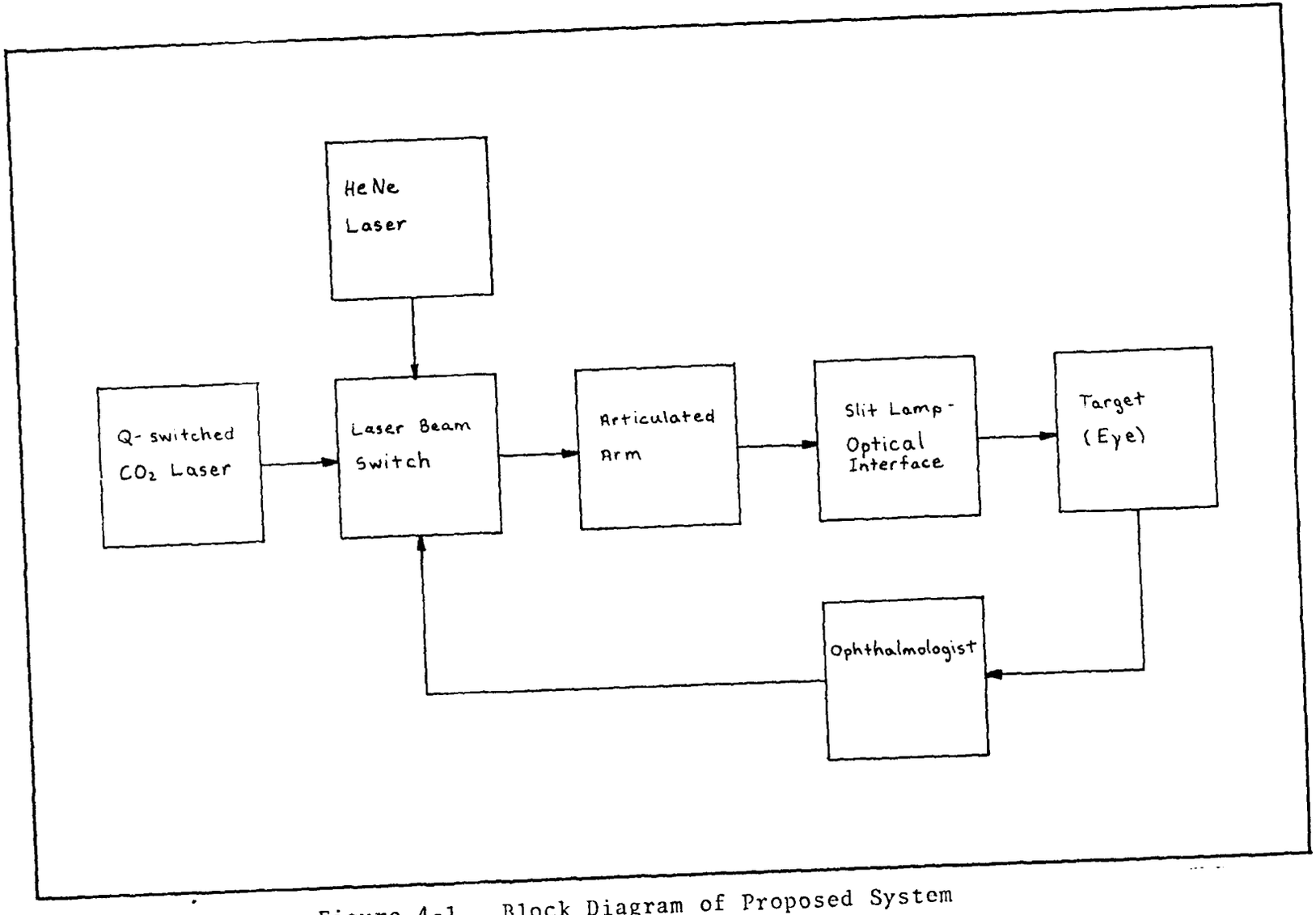

Figure 4-1. Block Diagram of Proposed System

of 10.6 μm. This radiation is ideal for making incisions within the cornea, since the cornea is opaque in the infrared region (0.77 μm to 250 μm). The CO_2 laser, employed in this research and pictured in Figure 4-2, is configured in the Q-switched mode. It exhibits a maximum average power output of 1.6 W and a peak power output of 597 W, with a pulse frequency of 10,000 Hz and a pulse duration of 500 ns. The laser beam has a far field spot diameter and a half-angle beam divergence of 6.3 mm and 1.1 mrad, respectively. In comparison, the "targeting" HeNe laser emits a continuous wave beam at a wavelength of 0.6328 μm and a power output of 1.4 mW. Its far field spot diameter and half-angle beam divergence are 0.488 mm and 0.825 mrad, respectively. A Nikon slit lamp was loaned to the school by the Ohio State University Eye Clinic. This slit lamp underwent considerable non-destructive modification in order to be integrated to the CO_2 and HeNe lasers. The slit lamp is shown in Figure 4-3.

Design

To successfully integrate these three commercially built components and produce a working laser-optical system, three custom components had to be designed and fabricated. These included a laser beam switch, an articulated arm, and an optical interface as previously illustrated in Figure 4-1.

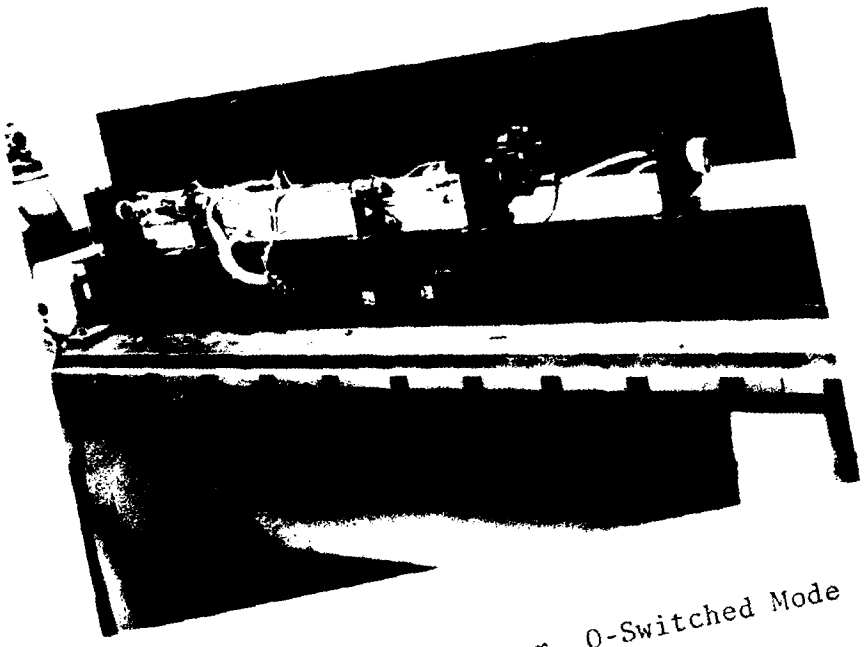

Figure 4-2. CO_2 Laser, Q-Switched Mode

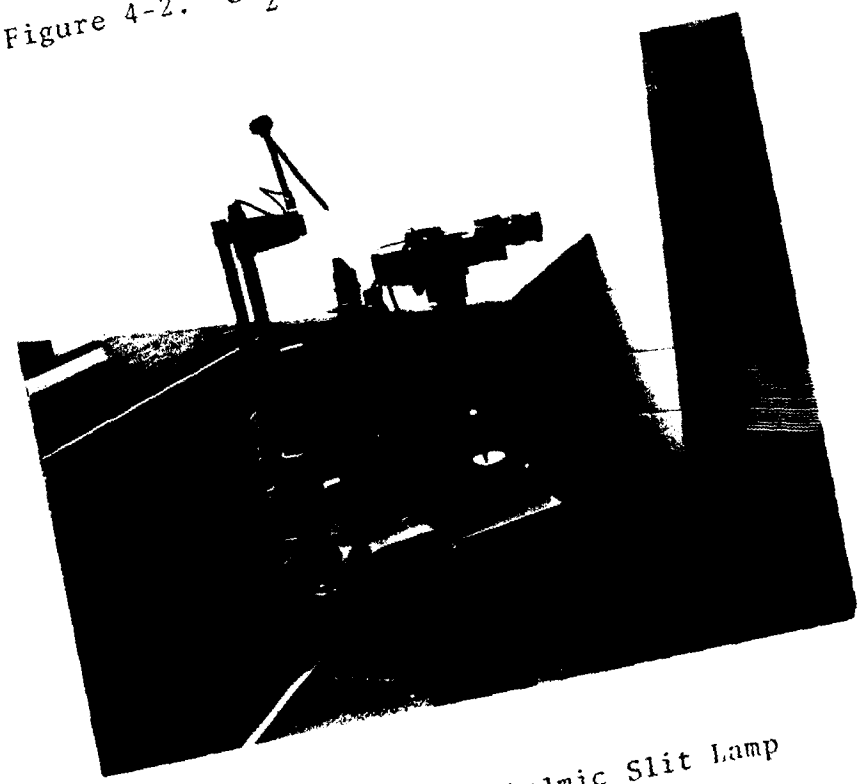

Figure 4-3. Ophthalmic Slit Lamp

Laser Beam Switch

The purpose of the laser beam switch is twofold. First, it serves to merge the CO_2 and HeNe laser beams coaxially for targeting. Second, it provides a surface from which to mount a neutral density filter. The neutral density filter intercepts only the HeNe beam and reduces its irradiance to a safe exposure level. Thus, the HeNe beam does not pose a risk to the eye of either the patient or ophthalmologist. It was desired to design a switch which was simple to operate, small in physical dimensions, rigid, and accurately alignable. An electrically actuated binary switch which passed either the CO_2 laser beam or HeNe laser beam was considered to be ideal.

With these features in mind, a switch as sketched in Figure 4-4 was constructed. Within the aluminum housing rests a pivotable and delicately balanced stainless steel mirror oriented at an angle of forty-five degrees to the incident, mutually perpendicular, CO_2 and HeNe laser beams. In the rest position, the actuator is off, the CO_2 beam is blocked, and the attenuated HeNe beam is reflected off the mirror surface and on through the optical system to the patient's eye. By depressing a foot switch, the ophthalmologist causes the actuator to trip the mirror, rotating it counter-clockwise, and holding it in a horizontal position until the foot switch is released. This action allows the CO_2 beam to pass through the switch unattenuated and

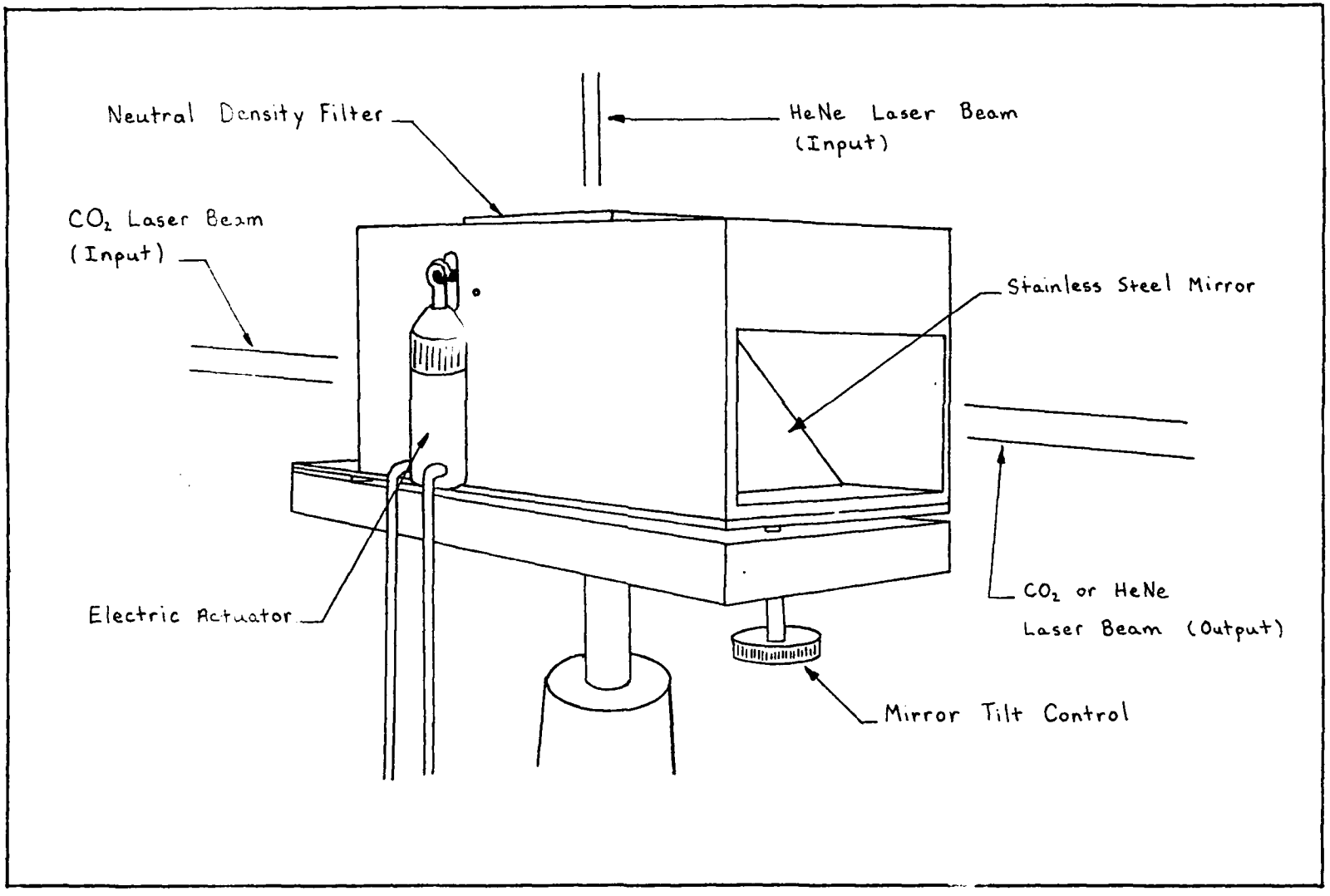

Figure 4-4. Laser Beam Switch

into the optical system where it is absorbed by the patient's cornea.

At the same time the HeNe beam is retroreflected from the mirror and passed back through the neutral density filter again. A highly polished stainless steel mirror was chosen for the reflector because of its high reflectivity, small coefficient of thermal expansion, strength, and resistance to oxidation. A detailed print of the laser beam switch is illustrated in Appendix B.

Articulated Arm

The major component needed in this system was a waveguide to direct laser energy from the beam switch to the slit lamp. Mobility was a critical factor which made the flexible articulated arm essential. The articulated arm's design was based upon articulated arms already used in medicine such as in the Sharplan laser (Ref 25). Full consideration was given to make the arm as light, yet strong, as possible. The arm required a diameter large enough to pass the CO_2 and HeNe laser beams, so it would not act as an aperture creating beam losses and unwanted spread through diffraction effects. In addition, the arm had to be totally enclosed as a safety precaution. The mirrors within the arm had to be composed of a material whose properties exhibited an ultra-high reflectance of CO_2 radiation, a high thermal conductivity coefficient, and a low linear expansion coefficient. Non-absorbent coatings should be used for preventing oxidation at the mirror surfaces.

If the mirrors did not exhibit high reflectance, then the arm's transmittance for CO_2 radiation would be low, reducing the beam power on the patient's eye to a point where cutting of corneal tissue could not be attained. The ultra-high reflectance criteria was not critical for the HeNe radiation because of the HeNe laser beam's role within the optical system. High thermal conductivity and low linear expansion coefficients were desired to ensure excellent heat dissipation and minimized thermal distortion of the mirror surfaces. Table 1 lists the reflecting metals considered for the mirrors during the selection process and the typical values of the pertinent properties (Ref 26 and 27:117). Copper was selected as the best material for the articulated arm's mirrors.

Table 1

Pure Metal Properties

Material	Reflectance (%)	Thermal Conductivity (BTU/hr/ft °F)	Linear Expansion µin/in °F
Aluminum	98.7	137	14
Silver	99.5	247	11
Gold	99.4	182	7.9
Copper	98.9	230	9.2
Rhodium	97.6	86.7	4.4

The finished articulated arm consisted of seven hardened aluminum optical elbows, each of which housed one copper mirror, all linked together by thin walled stainless steel tubing. Flexibility in the arm originated from five swivels properly located within the arm. An illustration of the arm is shown in Figure 4-5, and detailed prints are given in Appendix B. Three spring-loaded fine tuning adjustment screws are incorporated within each optical elbow so that the copper mirror in each can be pivoted. This feature allows each mirror to be precisely aligned with the optical axis of its optical elbow. If the mirrors are not precisely aligned, the laser beam will suffer serious misalignment as it travels through the arm. The swivels were designed to rotate smoothly, yet exhibit a tight fit. These features are achieved through the integration of high precision pin bearings and teflon spacers housed between the sleeve couplings and hollow shafts. The sleeve couplings unite the stainless steel tubing and the hollow shafts, which in turn are inserted within the appropriate optical elbows.

Optical Interface

The CO_2 and HeNe laser beams emitted from the articulated arm next enter the optical interface, which guides the radiation and focuses it onto the patient's eye. The optical interface contains the focusing optics whose theory of operation has already been presented in Chapter II. Structural

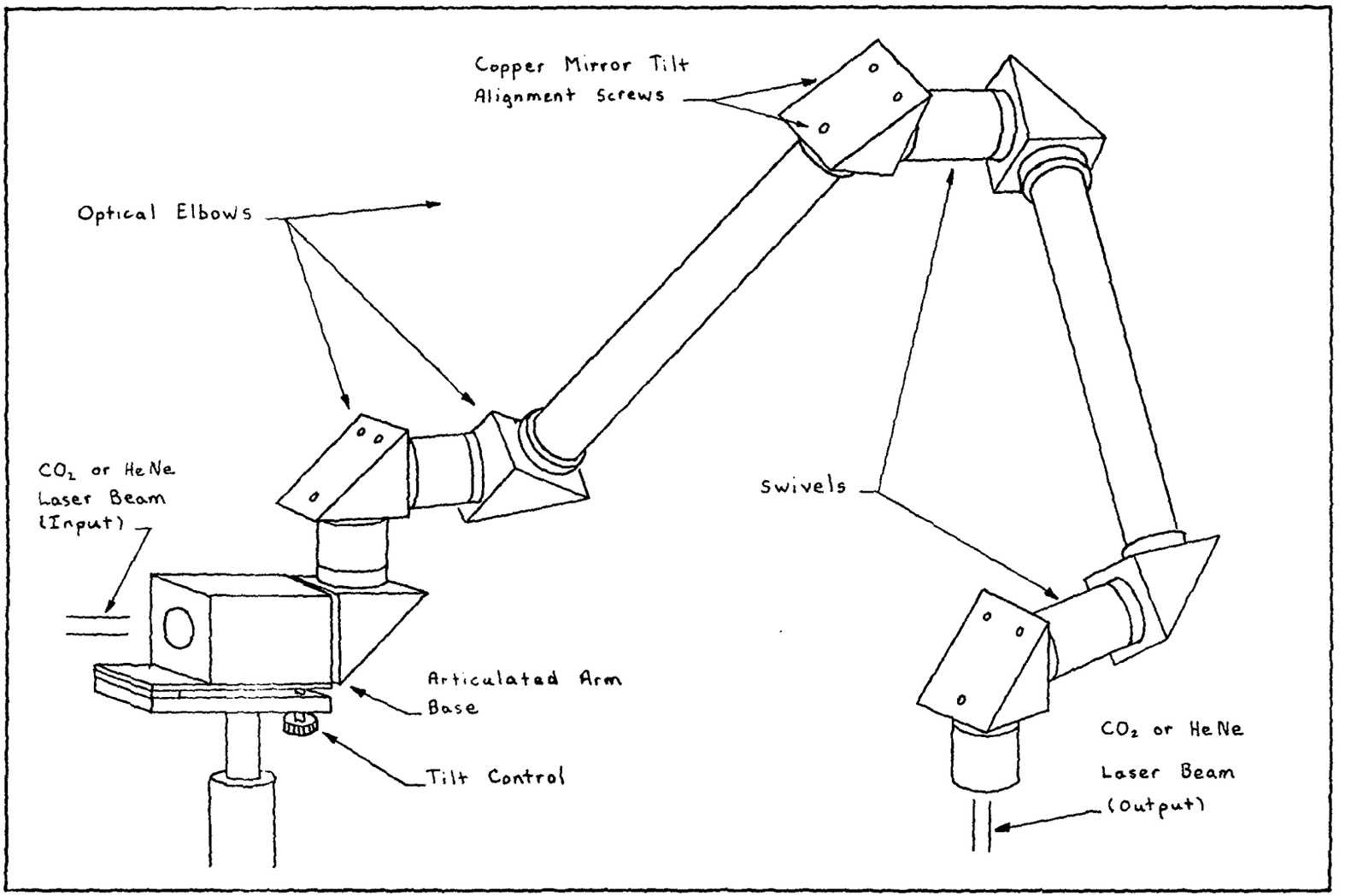

Figure 4-5. Articulated Arm

rigidity, high transmissivity, precise alignability of the optics, and microsurgical control of the laser beams were critical design considerations. Hardened aluminum was used in the fabrication of the optical interface's structure. As shown in Figure 4-6, within the interface are a large reflecting mirror, a commercially made Galilean beam expander and a meniscus lens. The beam expander is held in place by thumb screws which also serve to align it on the optic axis of the interface. The beam expander lenses are anti-reflection coated (at 10.6 μm) zinc selenide (ZnSe) -- one of the few water insoluble substances known to man which transmits both CO_2 and HeNe laser beams. The large copper mirror is mounted on a gimbal. It reflects the laser radiation passing through the beam expander onto the meniscus lens. The meniscus lens, in turn, focuses the expanded CO_2 laser beam onto the cornea of the patient. It is fixed on two sandwiched high precision mounts which move in directions perpendicular to one another. The transverse mounts enable the ophthalmologist to position the meniscus lens, relative to the patient's eye and the incident laser beam, in an accurate, optimal manner.

The interface attaches to the central post of the slit lamp by means of a spindle protruding from the interface's base. This configuration allows the interface to rotate smoothly about the central post, just as the white light source and binocular scope do on the slit lamp. With proper adjustment of the optical interface height, the object point

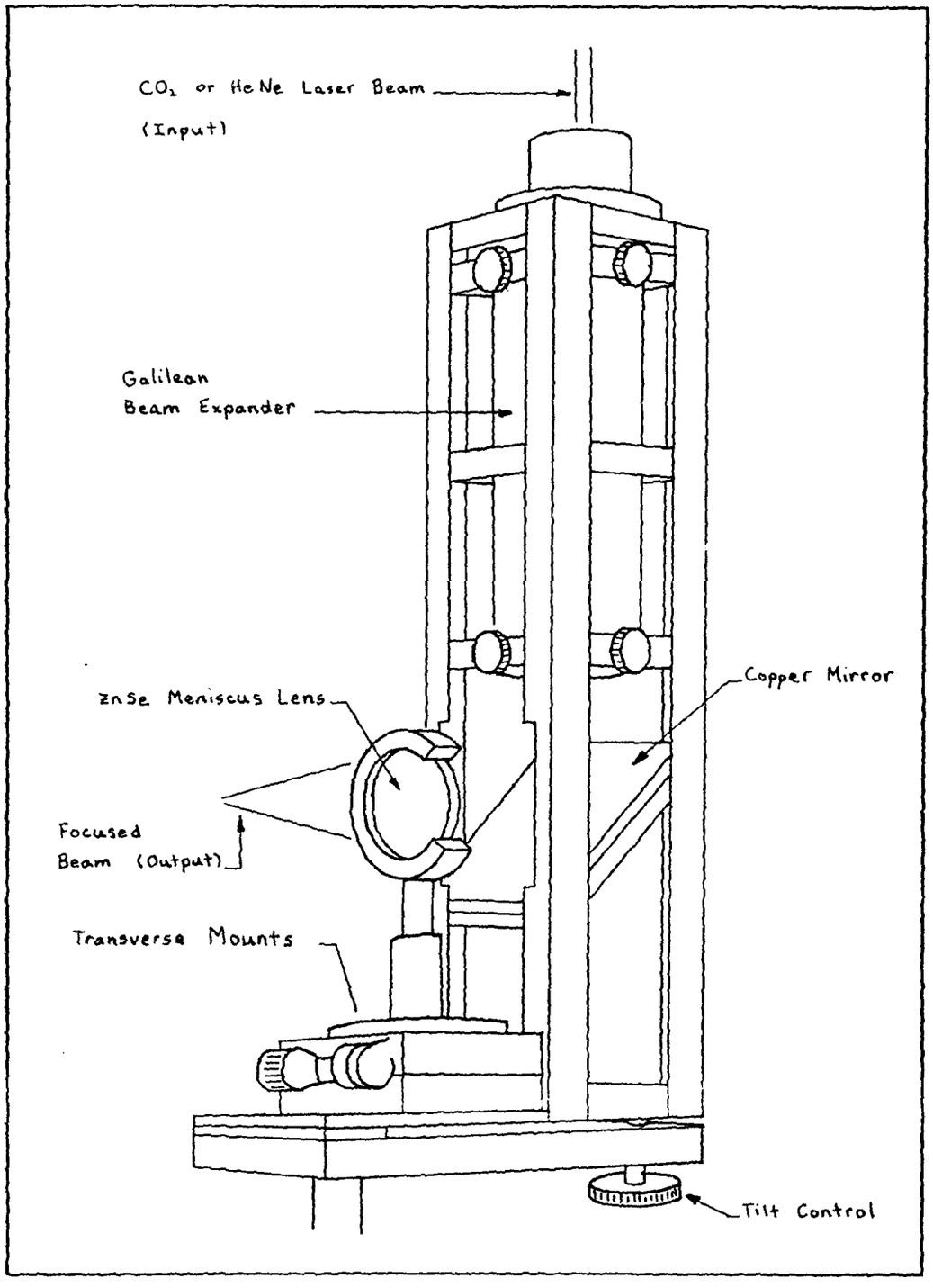

Figure 4-6. Optical Interface

as seen through the binocular scope and CO_2 focal point of the meniscus lens coincide. This is shown in Figure 4-7 which depicts how all of the system components integrate together, forming the desired final laser-optical system.

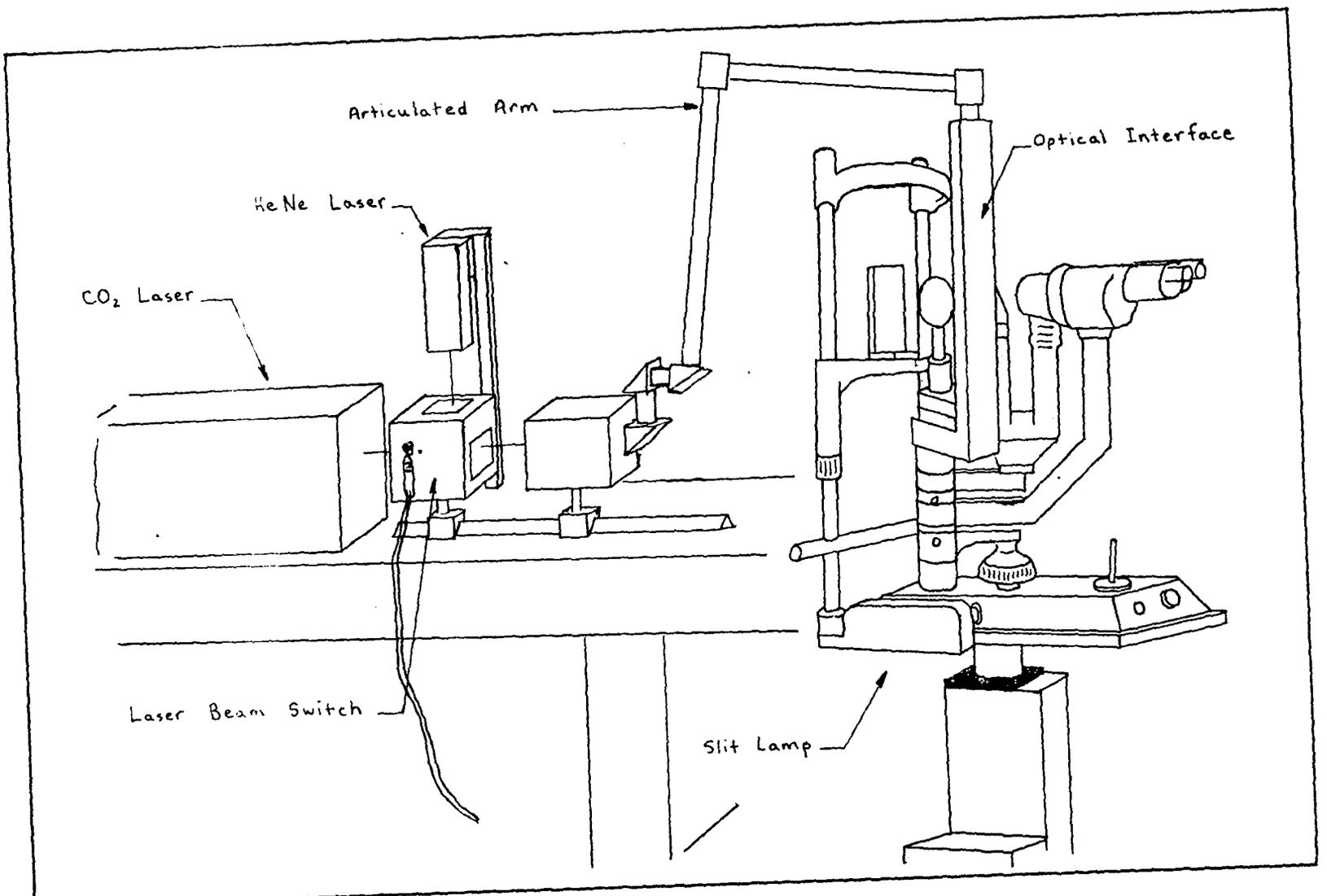

Figure 4-7. Designed Laser-Optical System

V. System Test and Evaluation

The information presented in this chapter addresses the diagnostics associated with the assembled laser-optical system, pictured in Figure 5-1. Several measurements and tests were performed to characterize the system's features and to evaluate its effectiveness as a laser scalpel for ocular procedures such as radial keratotomy.

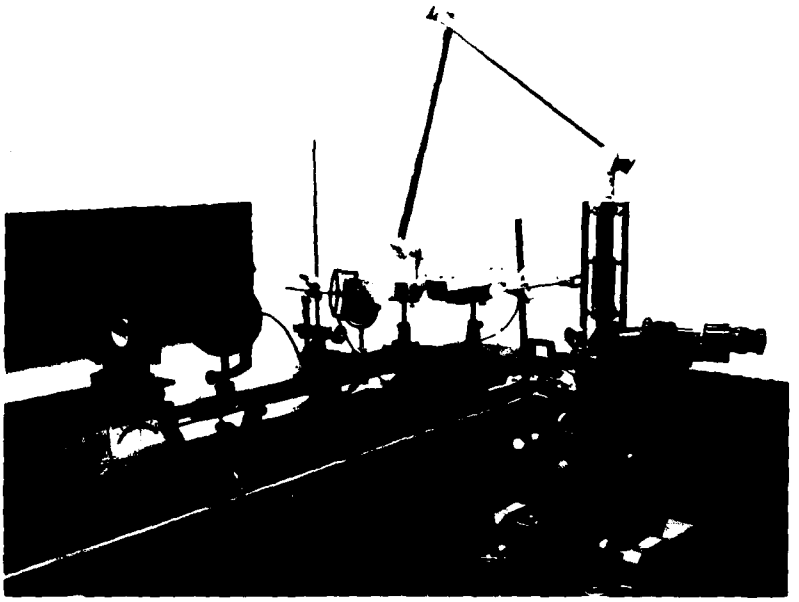

Figure 5-1. Assembled Laser-Optical System

Design Deficiencies

During the fabrication and final assembly of the optical system, a few unexpected problems developed. The first problem pertains to the laser beam switch. Though the component was machined and the electromagnetic switch operated flawlessly, the stainless steel mirror within the laser beam switch was not polished to acceptable standards. The unfortunate delay in correcting this defect prevented testing of the laser beam switch in the laser-optical system. A germanium window obtained from the AF Avionics Laboratory replaced the laser beam switch. Positioned at an angle of forty-five degrees relative to the incident, mutually perpendicular, CO_2 and HeNe laser beams, the germanium window coaxially merged the laser beams by transmitting the CO_2 radiation and reflecting the HeNe radiation, as shown in Figure 5-2. An electrically actuated shutter, fixed at the output of the germanium window, passed or blocked the entry of the laser beams into the attenuated arm and subsequently the optical interface. A second shutter, placed between the CO_2 laser and the germanium window, was used to block the CO_2 beam while the HeNe beam was focused onto the patient's cornea.

The major deficiency in the optical delivery system resides within the very delicate articulated arm. To operate correctly, the mirrors must be perfectly aligned so that the laser beam can be precisely guided along the contorted axis

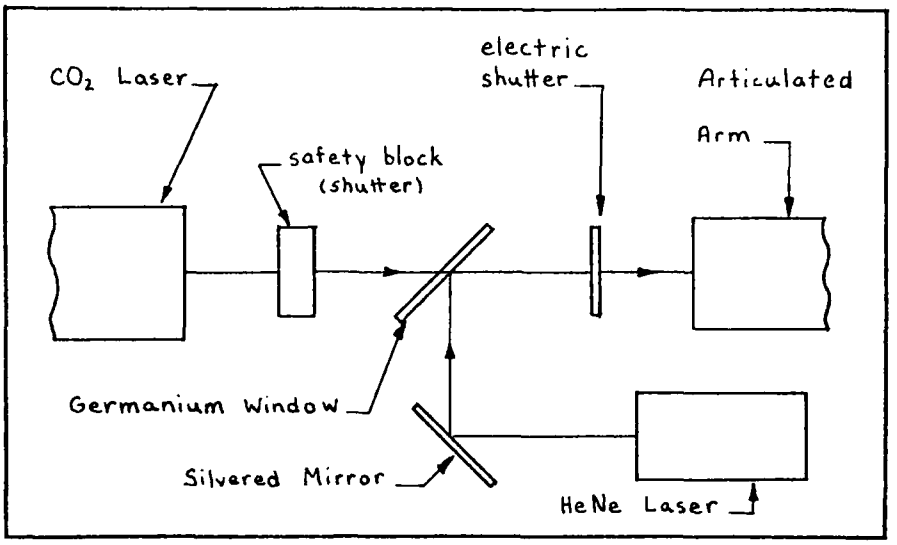

Figure 5-2. Germanium Window Assembly

of the arm. If a laser beam passing through an articulated arm does not remain coaxial with the optical axis of the arm, as the arm is arbitrarily moved, the final position of the laser beam focused on the target will be a function of the articulated arm's position. This result is highly unacceptable since the ophthalmologist must have accurate and predictable directional control of the laser beam. The articulated arm designed for this research study was subject to two shortcomings which caused the CO_2 and HeNe beams to move off the optical axis, at the arm's output, by as much as 0.5 cm. It was caused by the combination of slight twisting forces and bending moments incurred along the optical axis of the arm when the arm was moved. The heart of the problem can be traced to a somewhat less than massive base and to unacceptable "play" in the first two swivels. The tilt adjustment

screw and mounting pin located in the lower plate of the base introduced unwanted movement which interfered with the high rigidity required. The swivels developed a slight amount of play created by excessive tolerances in the pin bearings and minute buckling of the stressed metal tubing. As a temporary fix, it was decided to freeze the optical interface to the slit lamp -- which fixed the articulated arm in place -- and compensate for any misalignment by adjusting the arm's sixth and seventh mirrors. A moveable, vertically orientated platform, shown in Figure 5-3, was constructed and connected to the slit lamp in front of the final focusing lens -- before the experiments were conducted -- to position the test material in the CO_2 beam focal plane of the focusing lens. Horizontal cuts were obtainable, because the vertical orientated platform was free to move in directions transverse to the CO_2 laser beam.

In future designs, the problems encountered here will be corrected by engineering a more massive, rigid base; substituting hardened, thin walled, stainless steel tubing for the existing tubing; and replacing the pin bearings inside the swivels with lower tolerance, high precision, ball bearings mounted in thin races.

Optical System Transmittance

Before the optical system components were finally integrated, the transmittance of each component was measured to determine the total system transmittance. These

Figure 5-3. Vertical Platform

measurements pertained to both the HeNe and CO_2 laser beams. Table 2 contains the final results.

The transmittances for the overall system may appear low; however, these values are acceptable. First, safety considerations require the HeNe beam to be severely attenuated before it is focused onto a patient's eye. Thus, the low HeNe beam transmittance simply translates to the requirement for a weaker neutral density filter. Secondly, the CO_2 laser generates an ample amount of power in relation to that which is necessary for cutting corneal tissue; therefore, a low transmittance for the CO_2 beam is permissible.

Table 2		
Optical System Transmittances		
Component	Measured Transmittance	
	HeNe	CO_2
Articulated Arm	0.2643	0.7241
Beam Expander	0.4286	0.8984
Interface Mirror	0.6757	0.7619
Meniscus Lens	0.5714	0.9697
Germanium Window Assembly	0.9999	0.9913
Total System	0.0437	0.4764

HeNe Laser Focusing Diagnostics

The HeNe and CO_2 laser beams essentially share the same optical path even though the optical system is specifically designed for delivering and focusing the CO_2 beam onto the patient's eye. Since the refractive index of ZnSe is different for the HeNe and CO_2 laser beams ($n = 2.59$ for a wavelength of 0.6328 μm and $n = 2.40$ for a wavelength of 10.6 μm), it is clear that the focal planes of the meniscus lens for the highly collimated CO_2 and HeNe radiation cannot coincide. Employing the thin lens law, it can be shown that the HeNe

beam focuses 4.55 mm nearer to the meniscus lens than the CO_2 beam. This implies that the HeNe beam will spread to a somewhat larger diameter when it arrives at the focal plane of the CO_2 beam -- corneal surface. With a large HeNe beam spot diameter incident upon the cornea, the CO_2 beam will be more difficult to position accurately. This phenomenon was observed, in the assembled laser-optical system, on a white screen situated at the CO_2 beam focal plane of the meniscus lens. There, the HeNe beam produced a spot diameter 4.5 mm wide. Through a series of trials, neutral density filters with increasing optical densities were inserted within the system's optical path at the output of the HeNe laser. As the optical densities of the neutral density filters increased, the illuminance and spot diameters of the diverging HeNe beam decreased. The smallest detectable spot diameter was 2.1 mm wide. This experiment demonstrated that the CO_2 laser beam could not be optimally focused "on target" with the microscopic precision required in corneal surgery, by simply reducing the spot diameter of the diverging HeNe laser beam. Rather, to optimally focus the CO_2 laser beam on target, it is best to focus the HeNe beam on target first; then back the meniscus lens 4.55 mm farther away from the target. The target then resides in the CO_2 beam focal plane of the meniscus lens. Repeating the neutral density filter experiment a second time, now with the HeNe beam focused onto the white screen, it was observed that the attenuated HeNe beam was detectable so long

as the neutral density filter, within the system's optical path, did not exceed an optical density of 5.2. Adding a neutral density filter with an optical density of 5.2 to the system provides the required safety factor for both the patient and ophthalmologist.

CO_2 Laser Focusing Diagnostics

After the HeNe beam tests were performed, experiments were conducted on the laser-optical system's capability to focus CO_2 radiation. These tests were conducted to determine how well the focused beam could cut corneal tissue and whether the system could satisfy the man/machine interface requirements for ocular surgery. Three types of experiments were performed: irradiation of surgical sutures; cutting of plastic sheets; and finally, cutting of corneal tissue.

Irradiation of Surgical Suture

To determine CO_2 beam control for the final integrated system, 9-0 Ethicon surgical suture, backed by heat sensitive thermal paper, was attached to the moveable vertical platform. The suture was irradiated with different bursts of CO_2 energy by means of the electrically actuated, controllable shutter installed within the system's optical path. Several of the shots which were accurately targeted had sufficient energy to rupture the suture. An example of these results is depicted in the photograph of Figure 5-4. The laser power level and shutter speed settings which produced

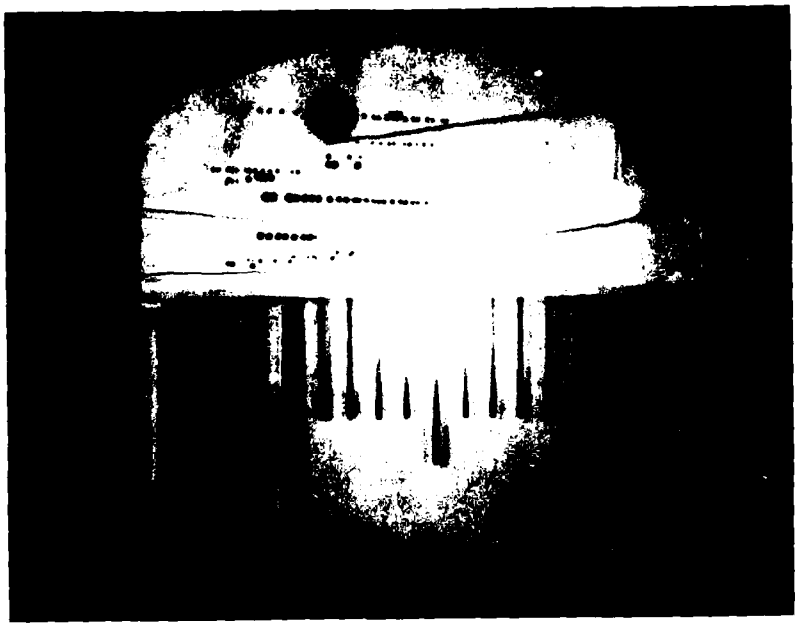

Figure 5-4. Ruptured Surgical Suture

ruptures most consistently were 0.5 W and 0.01 s, respectively. The energy deposited upon the suture with these settings, taking the overall optical system transmittance into account, is 2.4 mJ. On a few occasions the laser beam punctured a hole completely through the 50 μm diameter suture, but never severed it. The mean diameter of the holes was 25 μm. Holes burned through the thermal paper from shots intentionally focused on it and not the suture averaged 23 μm wide. It is reasonable to assume that the widths of the holes are equal in size to the focused laser beam spot diameter. The Rayleigh range which corresponds

to an average spot diameter of 23 μm is approximately 39 μm. This compares well to the theoretically predicted Rayleigh range of 14.7 μm and spot diameter of 16 μm calculated in Chapter II.

Irradiation of Plastic Sheets

Plastic sheets were irradiated with the focused CO_2 laser beam to obtain preliminary indications on the size of incision widths that could be expected and the laser power outputs necessary to produce them. The plastic sheets overlayed thermal paper which was backed by white cardboard. These targets were then individually attached to the moveable platform where they were situated in the CO_2 focal plane of the meniscus lens. Several tests were conducted with the CO_2 laser power ranging from 0.1 W to 1.5 W. These values, when considering the total optical system transmittance, yielded power values at the plastic sheets extending from 0.048 W to 0.715 W, respectively. For each established power level, two incisions were made by moving the targets on the moveable platform across the focused CO_2 laser beam. The moveable platform was restricted to a transverse speed of 0.5 cm/s. In each test, the first incision was made with only one sweep of the beam, and the second was made from ten consecutive sweeps. After several runs, it was determined that the best incision (narrowest and deepest) occurred at a laser power level of 0.3 W --

0.144 W working power at the surface of the plastic sheet. The incision width made from one sweep at this setting was 24 μm wide, and the cut nearly penetrated the 50 μm thick plastic sheet. The incision width produced by ten sweeps of the laser beam, at this power setting, was measured to be 83 μm and the cut clearly penetrated the plastic sheet. In all cases, it was found that increasing the number of sweeps also increased the width and depth of a cut, most notably the depth.

Irradiation of Corneal Tissue

The ultimate test of the laser-optical system was to cut corneal tissue and evaluate its ability to produce microscopic incisions that would be acceptable for corneal surgery, particularly radial keratotomy. Pig eyes, obtained from a local abattoir, were used as a source for corneal tissue. Pig corneas were selected as the test material because of their biological similarity to the human cornea. Prior to cutting, the enucleated eyes were mounted on the moveable platform, as shown in Figure 5-5.

The CO_2 laser beam was focused onto the vertical centerline of each pig cornea by focusing the HeNe beam onto the cornea first, and then backing the meniscus lens 4.55 mm farther away from the respective cornea. It was discovered that, while focusing the attenuated HeNe beam onto the cornea, the reflectance of the HeNe beam from the

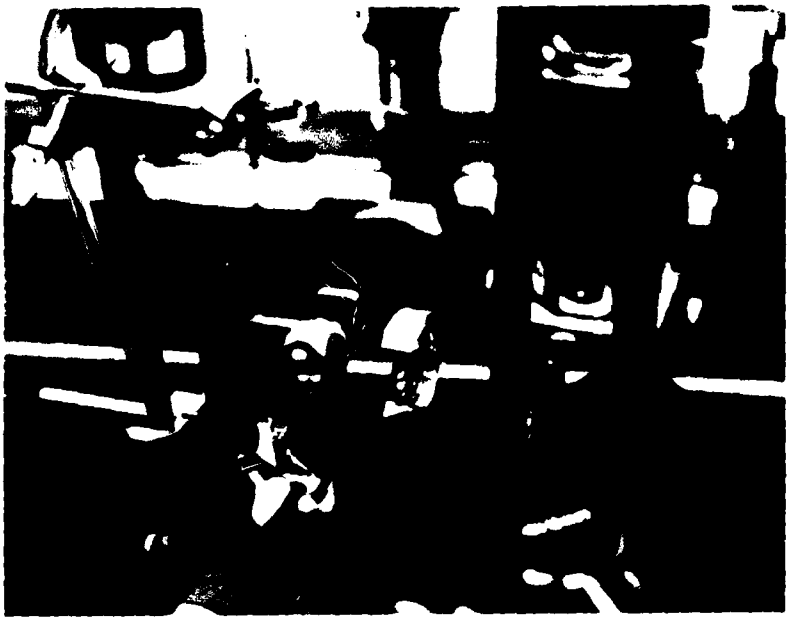

Figure 5-5. Pig's Eye Attached to Vertical Platform

corneal surface was low and the transmittance through the cornea was high. To clearly visualize the focused HeNe beam spot on the corneal surface, it was required that the neutral density filter in this optical system have an optical density value less than two, a value which is considered unsafe according to the calculations given in Chapter II.

A variety of CO_2 laser power output settings were employed to cut the pig corneas. Horizontal incisions were cut at a speed of approximately 0.5 cm/s. Incisions were consistently made with CO_2 laser power output settings

greater than 0.4 W which corresponds to a working power of 0.19 W incident upon the cornea. Slight charring and opaqueness of the corneal tissue was evident at the edges of the incisions. Increased CO_2 beam power led to deeper cuts within the corneal tissue, but the increased power also increased the amount of charring and opaqueness of the tissue surrounding the cut. Retracing the cuts appeared to make the incisions deeper, but at the same time made them wider. The corneal incisions measured approximately 1.0 cm long. The cuts were limited in length due to the curvature of the cornea, which carried the surface at the periphery of the cornea beyond the Rayleigh range of the focused CO_2 laser beam. An example of an incision is sketched in Figure 5-6.

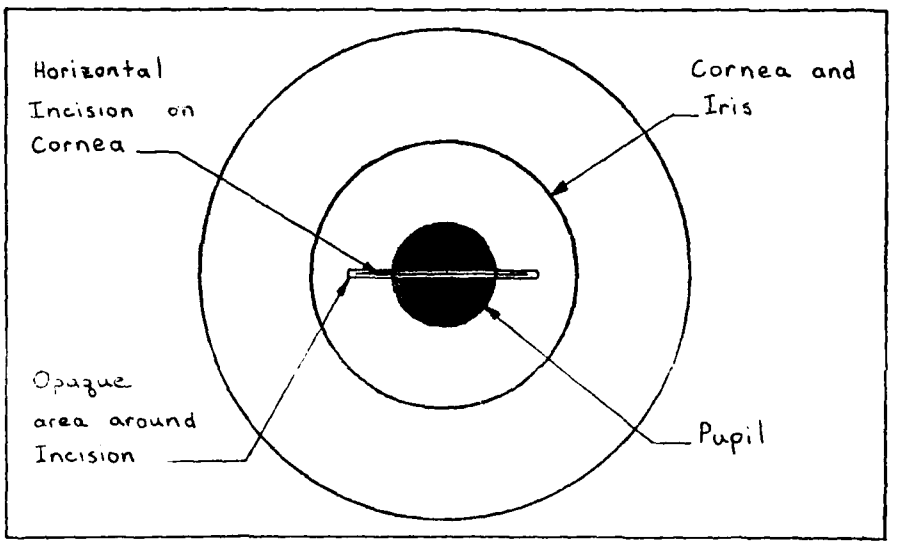

Figure 5-6. Corneal Incision

Dr. Richard H. Keates, senior ophthalmologist from the Ohio State University Eye Clinic, highly experienced in radial keratotomy and laser research in ophthalmology, visited the laboratory and tested the laser scalpel. Using a pig eye for a test material source, Dr. Keates cut a few incisions within the cornea at working power output settings of 0.33 W and 0.38 W. Two incisions were made from a single sweep and one incision was made from four sweeps of the CO_2 laser beam. Analysis of the results within the laboratory correlated well with incisions made in earlier tests. The widths of the corneal incisions formed by the CO_2 laser beam were comparable to the incision widths made in human corneas, with special metal scalpels, during actual radial keratotomies. A clinical analysis of the corneal incisions was performed at the Ohio State University Eye Clinic; however, the results were not available for release at the time of this writing.

VI. Conclusions and Recommendations

Conclusion

A laser-optical system, yielding a 23 μm spot diameter at the system output and exhibiting micro-precision beam controllability, was designed, fabricated, tested and evaluated. The purpose of this system is to provide ophthalmologists with a safe surgical instrument which delivers high power CO_2 laser radiation to a patient's eye for treatment of ocular disorders and diseases, particularly myopia. The CO_2 laser was chosen because of the cornea's complete absorption of 10.6 μm radiation. The final system primarily consisted of a Q-switched CO_2 laser source and a standard ophthalmic slit lamp optically connected together by an articulated arm and optical interface. An attenuated HeNe laser source delivering an output beam coaxially located with the CO_2 laser beam, by way of proper positioning of a germanium window, was incorporated in the laser-optical system to optimally target and focus the CO_2 laser beam onto the test materials.

Diagnostics were performed to determine the efficacy of the laser scalpel. Transparent plastic sheets, 9-0 Ethicon surgical suture, and pig corneas were irradiated with the sharply focused CO_2 radiation. Incisions produced in the plastic sheets, produced by a single sweep of the CO_2 laser beam, exhibited widths as narrow as 24 μm.

Preliminary analysis of incisions cut within corneal tissue by the CO_2 radiation concluded that the widths of the incisions were comparable to the incision widths made in human corneas with special metal scalpels during actual radial keratotomies. Results from a clinical analysis of the CO_2 laser induced corneal incisions were not available at the time of this writing. To demonstrate beam control, 50 μm wide surgical suture was severed with bursts of CO_2 energy. In some cases, 25 μm holes were punched through the suture without rupturing it. Consistent severing of suture occurred with an energy deposition of 2.4 mJ.

To complement the design project, comprehensive calculations were performed to help ophthalmologists select optimal spot diameter and Rayleigh range values of medical lasers to maximize the success of the patient's postoperative recovery. The calculations addressed five different lasers: CO_2, Nd^{3+}:YAG, Ruby, Argon, and KrF*. The CO_2 laser exhibits the shortest Rayleigh range, for any given spot diameter, regarding the five lasers studied. As the CO_2 beam is focused to smaller spot diameters, the Rayleigh range rapidly approaches values having the same order of magnitude as the corresponding spot diameters. A short Rayleigh range impedes the cutting of deep incisions. In contrast, the KrF^* laser, of the five lasers studied, displays the longest Rayleigh range for any given spot diameter. The KrF^* laser may be ideally suited for ocular surgery since much of the ocular media absorbs ultraviolet radiation.

Recommendations

During the assembly or development testing of many first generation systems, shortcomings usually show up. This research project was not any different; unfortunately, the remaining time was too short to implement engineering changes. Before this laser-optical system can meet its originally intended design capability, a few fabrication and engineering actions must be taken.

A germanium window covered with an anti-reflection coating for randomly polarized 10.6 μm CO_2 laser radiation, incident at an angle of 45°, should be purchased for the laser-optical system to replace the borrowed germanium window.

The copper mirrors should all be repolished to remove any oxidation, especially the large optical interface mirror which has numerous scratches and digs. After the mirrors are polished, they should be coated to maximize and retain their reflectance for CO_2 laser radiation. In the event that the mirrors are not polished, then they should be replaced with new copper or dielectric mirrors having a flatness of at least $\lambda/10$, and coated to retain their ultra-high reflectance of 10.6 μm CO_2 radiation, incident at an angle of 45°.

It would be ideal to replace the articulated arm with a flexible fiber optic cable; however, until a fiber optic cable is available, the laser-optical system must incorporate the articulated arm. For the existing arm, a few

engineering changes are required to hold the laser beams on the contorted axis. The arm's base should be redesigned so that there is no rotation at its post. It should not incorporate a tilt control, otherwise twisting and bending moments will persist. The thin walled stainless steel tubing, which links the optical elbows and swivels together, ought to be hardened or replaced with hardened thin walled stainless steel tubing. The pin bearings which fit inside the arm's swivels should be replaced with lower tolerance, high precision ball bearings mounted in thin races. These changes, if implemented, will keep the CO_2 and HeNe laser beams on the contorted axis of the arm while it is moved, letting the laser-optical system achieve its design performance.

Last of all, a study should be conducted to determine the thermal conductivity and measure the local temperature changes in the cornea following CO_2 laser irradiation. These topics must be thoroughly understood before the CO_2 laser can be used as a laser scalpel in ocular surgery.

Bibliography

1. Landers, M.B. III et al. "The Current Status of Laser Usage in Ophthalmology," in Third Conference on the Laser, edited by L. Goldman. New York: New York Academy of Sciences, 1975.

2. Wolbarsht, M.L. and M.B. Landers. "Lasers in Ophthalmology: The Path from Theory to Application," Applied Optics, 18 (10): 1518-1526 (May 15, 1979).

3. Schwartz, L.W. et al. "Argon Laser Iridotomy in the Treatment of Patients with Primary Angle-Closure or Pupillary Block Glaucome: A Clinicopathological Study," Ophthalmology (Rochester), 83 (3): 294-309 (March 1978).

4. Rodrigues, M.M. et al. "Argon Laser Iridotomy on Primary Closure of Pupillary Block Glaucoma," Archives of Ophthalmology," 96 (12): 2222-2230 (December 1978).

5. Schwartz, A.L. et al. "Argon Laser Trabecullar Surgery in Uncontrolled Phakic Open Angle Glaucoma," Ophthalmology (Rochester), 88 (3): 203-212 (March 1981).

6. Goldman, L. "Laser in Medicine," CRC Applications of the Laser, Cleveland: CRC Press, Inc., 1973.

7. L'Esperance, F.A., Jr. "Photocoagulation with the Frequency Doubled Nd:YAG," American Journal of Ophthalmology, 71: 631-638 (March 1971).

8. Rosa, D. et al. "Use of the Neodymium-YAG Laser to Open the Posterior Capsule after Lens Implant Surgery: A Preliminary Report," Journal of the American Intraocular Implant Society, 6 (4): 352-354 (October 1980).

9. Karlin, D.B. et al. "CO_2 Laser in Vitreoretinal Surgery: 1. Quantitative Investigation of the Effects of CO_2 Laser Radiation on Ocular Tissue," Ophthalmology, 86 (2): 290-298 (February 1979).

10. Beckman, H. et al. "Carbon Dioxide Laser Surgery of the Eye and Adnexa," Ophthalmology, 83 (10): 990-1000 (October 1980).

11. Fyodorov, S.N. and V.V. Durnev, "Operation of Dosaged Dissection of Corneal Circular Ligament in Cases of Myopia of Mild Degree," Annals of Ophthalmology, 1885-1890) (December 1979).

12. Schacher, R.A. et al. "A Physicist's View of Radial Keratotomy with Surgical Implications," Keratorefraction, edited by R.A. Schacher, et al. Denison TX: LAL Publishing, 1980.

13. Kramer, S.G. et al. "Precision Standardization of Radial Keratotomy," Ophthalmic Surgery, 12 (8): 561-566 (August 1981).

14. Barnes, F.S. "Applications of Lasers to Biology and Medicine," Proceedings of the IEEE, 63 (9): 1269-1278 (September 1975).

15. Geeraets, F.S. and E.R. Berry. "Ocular Spectral Characteristics as Related to Hazards from Lasers and Other Light Sources," American Journal of Ophthalmology, 66 (1): 15-20 (July 1968).

16. Boettner, E.A. and J.R. Walter. "Transmission of the Ocular Media," 6570 Aerospace Medical Research Laboratories, Wright-Patterson AFB OH, Technical Documentary Report No. MRL-TDR-62-63 (May 1962).

17. Keates, R.H. et al. "Carbon Dioxide Laser Beam Control for Corneal Surgery," Ophthalmic Surgery, 12 (2): 117-122 (February 1981).

18. Weichel, H. and L.S. Pedrotti, "A Summary of Useful Laser Equations - An LIA Report," Electro-Optical Systems Design, 8: 22-32 (July 1976).

19. Yariv, A. Introduction to Optical Electronics, New York: Holt, Rinehart and Winston, 1976.

20. Siegman, A.E. An Introduction to Lasers and Masers, New York: McGraw-Hill, 1971.

21. AFM 161-32.

22. AFR 161-24.

23. 900 Argon Laser Photocoagulator. Operator's Manual. Palo Alto CA: Coherent Medical Division.

24. Harrington, J.A. "Crystalline Infrared Fibers," Proceedings of the SPIE, 266: 10-15 (Spring 1981).

25. Kaplan, I. "The Sharplan 791 CO_2 Surgical Laser in Clinical Surgery," Laser 77 Opto-Electronics Conference Proceedings, edited by W. Waidelich. England IPC Science and Technology Press, Ltd., 1977.

26. American Institute of Physics Handbook, Third Edition, Copyright 1972.

27. Handbook of Tables for Applied Engineering Science, Second Edition, Copyright 1973.

APPENDIX A

Computer Program and Sample Results of Spot Diameter and Rayleigh Range Dependence on Wavelength, Calculations

The computer program, mentioned in Chapter III, which calculates the theoretical spot diameters and corresponding Rayleigh range values for the five different lasers (CO_2, Nd^{3+}:YAG, ruby, argon and KrF*) is presented in this appendix. The program, written in Control Data Corporation's Fortran Version 5 computer language, runs through 'K' complete cycles, each of which pertains to a different wavelength fed into the computer from a punched card. Thus, for example, if the spot diameter and Rayleigh range values for six different lasers is desired, set the variable 'K' in the program equal to six, and include six input cards characterizing the chosen wavelengths. No special format for the input cards is necessary, because the computer program is written to let the computer determine the appropriate format used. Cal-comp plotter commands are included within the program to produce a graph of the final results.

The computation process begins by generating a limited range of f/d_{01} values for the focusing lens. This quotient represents the ratio of the converging lens focal length to the incident laser beam spot diameter on the lens. Practical values for the ratio f/d_{01} were chosen to range from one to

twenty in increments of one-eighth. Focused spot diameters were calculated using Eq (3) and were truncated at a maximum value of 42 μm for cal-comp plots. Corresponding values of Rayleigh range were then calculated using Eq (6) and likewise truncated to 120 μm. The following is a listing of the computer program and sample results.

```
      PROGRAM FOFM
      DIMENSION SD(1 2),Z(152),FD(1  ),F1(1E )
C
C     PURPOSE:  THIS FIGURE OF MERIT ALGORITHM IS A TOOL INTENDED TO FACILITATE
C     SURGEONS IN CHOOSING THE OPTIMAL LASER (REGARDING WAVELENGTH, AND MENISCUS
C     LENS FOCAL LENGTH, GIVEN THE LASER BEAM'S SPOT DIAMETER) FOR ANY OCULAR
C     SURGICAL  PROCEDURE.
C
      CALL PLOT(1.5,1.5,-3)
      CALL FACTOR(.777)
      K=5
      L=
      SD(1 1)=  .
      Z(151)=  .
      SD(1 2)=7.
      Z(152)=15.
      CALL AXIS( .5, . ,'SPOT DIAMETER (MICRONS)',23,6.5,90.0,SD(151),SD
     1(152))
      CALL AXIS( . , . ,'RAYLEIGH RANGE (MICRONS)',-2 ,8.5,90.0,Z(151),Z(
     1152))
   32 READ(*,*,END=8 )WL
      DO 4  I=1,15 ,1
      FD(I)=(I+7. )/2.
      SD(I)=4. *WL*FD(I)/3.141592654
      Z(I)=(3.141592654*SD(I)**2. )/(4.*WL)
      FM(I)=Z(I)/SD(I)
   4  CONTINUE
      WL=WL*1.E5
      WRITE(*,3 )WL
   3  FORMAT(' ','FOR A WAVELENGTH OF',1X,F8.4,1X,'MICRONS.')
      WRITE(*,34)
   34 FORMAT(' ',8X,'F/D',5X,'SPOT DIAMETER',2X,'RAYLEIGH RANGE',5X,'FIG
     1URE OF MERIT')
      WRITE(*,36)
   36 FORMAT(' ',19X,'(MICRONS)',6X,'(MICRONS)')
      DO 7  J=1,15 ,1
      SD(J)=SD(J)*1.  E5
      Z(J)=Z(J)*1.  E5
      WRITE(*,38)FD(J),SD(J),Z(J),FM(J)
   38 FORMAT(' ',6X,F6.3,6X  3,7X,F1 .3,11X,F7.3)
      IF(SD(J).GT.42.3.OR  Z  GT.12. ) THEN
      SD(J)=SD(J-1)
      Z(J)=Z(J-1)
       ND IF
   7  CONTINUE
      CALL LINE(Z,SD,15 ,1,0, )
      L=L+1
      IF(L .LT.K) GO TO 32
      CALL PLOTE(DUM)
   99 GO T  72
   8  STOP
      END
```

Copyright ... permitted ... not

FOR A WAVELENGTH OF [illegible] MICRONS.

F/D	SPOT DIAMETER (MICRONS)	RAYLEIGH RANGE (MICRONS)
1.[illegible]	13.[illegible]	13.495
1.125	1[illegible].183	17.331
1.25	1[illegible].97	21.[illegible]68
1.375	1[illegible].157	25.517
1.[illegible]	2[illegible].24	3[illegible].367
1.[illegible]25	21.932	35.639
1.[illegible]75	2[illegible].619	41.383
1.875	2[illegible].31[illegible]	47.448
2.[illegible]	28.993	53.855
2.125	2[illegible].68	6[illegible].9[illegible]4
2.25[illegible]	3[illegible].36[illegible]	68.325
2.375	32.[illegible]	75.128
2.[illegible]5	33.741	84.352
2.625	3[illegible].[illegible]23	92.958
2.751	37.115	1[illegible]2.[illegible]66
2.875	3[illegible].[illegible]12	111.555
3.[illegible]	[illegible].789	121.[illegible]67
3.125	[illegible]2.175	131.8[illegible]
3.25[illegible]	[illegible]3.863	1[illegible]2.555
3.375	45.95	153.732
3.[illegible]	[illegible]7.237	16[illegible].33[illegible]
3.[illegible]25	[illegible]8.92[illegible]	177.35[illegible]
3.751	[illegible].611	189.792
3.875	52.29[illegible]	2[illegible]2.655
[illegible]	[illegible]3.98[illegible]	215.941
[illegible].125	[illegible]5.672	229.6[illegible]9
[illegible].25[illegible]	57.353	2[illegible]3.778
[illegible].375	58.[illegible]6[illegible]	256.328
[illegible].[illegible]	6[illegible].3[illegible]	273.3[illegible]1
[illegible].625	62.[illegible]21	288.695
4.75[illegible]	6[illegible].133	3[illegible]4.511
[illegible].875	6[illegible].79[illegible]	32[illegible].7[illegible]9
5.[illegible]	67.[illegible]82	337.[illegible]8
[illegible].125	[illegible]8.15[illegible]	3[illegible].[illegible]9,
[illegible].[illegible]5[illegible]	7[illegible].5[illegible]5	3[illegible]1.39[illegible]
[illegible].77[illegible]	[illegible]2.5[illegible]3	3[illegible]9.91[illegible]
[illegible].[illegible]5[illegible]	7[illegible].[illegible]3	[illegible]8.2[illegible]+
5.[illegible]2[illegible]	79.[illegible]1[illegible]	[illegible]2[illegible].[illegible]33
5.751	77.[illegible]14	446.223
5.[illegible]75	7[illegible].29[illegible]	[illegible]6[illegible].[illegible]7[illegible]
5.[illegible]875	[illegible]7.97[illegible]	[illegible]0[illegible].5[illegible]8
6.[illegible]	[illegible]2.[illegible]6[illegible]	[illegible].[illegible].3[illegible]4
6.125	[illegible]1.352	527.2[illegible]1
6.25[illegible]	[illegible]6.[illegible]3[illegible]	[illegible]0.[illegible][illegible]
6.375	[illegible]6.[illegible]3[illegible]	[illegible]7.[illegible]2[illegible]
6.[illegible]	[illegible]7.[illegible]26	[illegible]7.[illegible]2[illegible]
6.[illegible]25	[illegible]8.[illegible]17	592.333
6.[illegible]5[illegible]	[illegible]1.[illegible]3	[illegible]14.927
6.[illegible]75	[illegible]2.[illegible]8[illegible]	637.913

Reproduction not

FOR A WAVELENGTH OF .2[illegible] MICRONS.

F/D	SPOT DIAMETER (MICRONS)	RAYLEIGH RANGE (MICRONS)
1.[illegible]	.31[illegible]	.318
1.12[illegible]	.35[illegible]	.4[illegible]3
1.25[illegible]	.39[illegible]	.4[illegible]87
1.37[illegible]	.[illegible]3[illegible]	.5[illegible]2
1.[illegible]	.[illegible]7[illegible]	.716
1.62[illegible]	.[illegible]1[illegible]	.8[illegible]1
1.75[illegible]	.[illegible]5[illegible]	.975
1.87[illegible]	.[illegible]9	1.119
2.[illegible]	.[illegible]3[illegible]	1.273
2.125	.[illegible]7[illegible]	1.437
2.25[illegible]	.715	1.611
2.375	.756	1.795
2.[illegible]1	.79[illegible]	1.989
2.625	.83[illegible]	2.193
2.75[illegible]	.875	2.4[illegible]7
2.875	.919	2.631
3.[illegible]1	.9[illegible]	2.865
3.125	.99[illegible]	3.1[illegible]8
3.25[illegible]	1.[illegible]35	3.362
3.375	1.[illegible]7[illegible]	3.625
3.5[illegible]	1.11[illegible]	3.899
3.625	1.15[illegible]	4.183
3.75	1.19[illegible]	4.478
3.875	1.233	4.781
4.[illegible]	1.27[illegible]	5.093
4.125	1.313	5.416
4.25	1.35[illegible]	5.7[illegible]3
4.375	1.393	6.093
4.5[illegible]	1.432	6.446
4.625	1.472	6.8[illegible]9
4.75	1.512	7.182
4.875	1.[illegible]52	7.565
5.[illegible]	1.592	7.953
5.125	1.631	8.361
5.25	1.671	8.773
[illegible].375	1.711	9.195
[illegible].[illegible]	1.751	9.623
[illegible].125	1.[illegible]9	[illegible].[illegible]72
5.[illegible]5[illegible]	1.[illegible]3	1[illegible].524
[illegible].[illegible]75	1.[illegible]7	1[illegible].[illegible]87
6.[illegible]	1.91	11.4[illegible]9
6.125	1.[illegible]5	11.842
6.25	1.[illegible]8[illegible]	12.434
[illegible].375	2.[illegible]2[illegible]	12.936
6.[illegible]	2.[illegible]8[illegible]	13.4[illegible]3
6.[illegible]25	2.1[illegible]8	13.971
6.75[illegible]	2.14[illegible]	14.[illegible]5[illegible]3
6.[illegible]75	2.18[illegible]	15.[illegible]4[illegible]5
7.[illegible]	2.22[illegible]	15.997
7.125	2.26[illegible]	16.[illegible]59
7.25[illegible]	2.3[illegible]	16.731
7.37[illegible]	2.34[illegible]	17.313

APPENDIX B

Detailed Prints of the Laser Beam Switch Articulated Arm and Optical Interface

In this appendix are the engineering drawings of the custom made laser beam switch, articulated arm, and optical interface designed for the laser-optical system by the author. The components, excluding the meniscus lens, the transverse mounts for positioning the meniscus lens, and the beam expander, were expertly machined by Mr. Russel Murray and Mr. David Paine of the AFIT Fabrication Shop. Mr. Bob Bertke polished the copper mirrors in the Air Force Materials Laboratory. A redesign of the articulated arm base and swivels, for correcting the laser-optical system's ailments, is included in these engineering drawings.

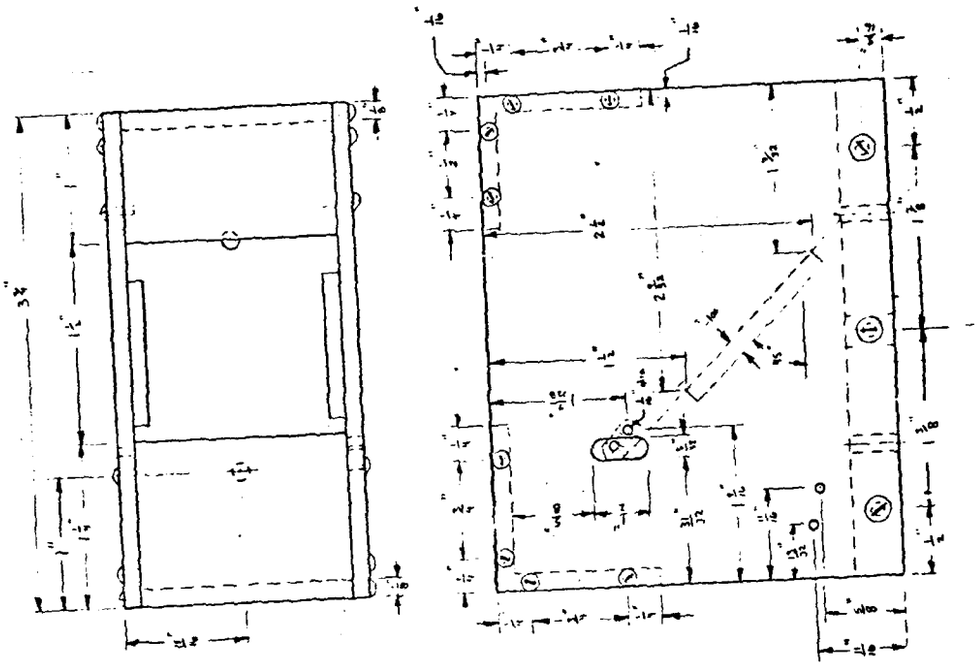

Laser Beam Switch Housing
design: LT O T PRASKA
AFIT GEO-81D
Aug 81

True scale
tolerances: ± .002"
material: aluminum

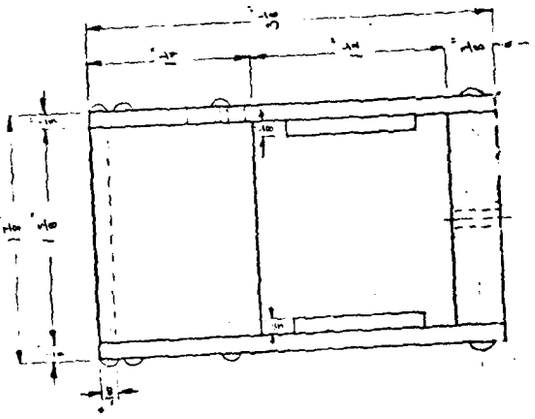

Mirror Assembly for
Laser Beam Switch

design : LT D J PRASKA
AFIT GED-81D
Aug 81

material : stainless steel
tolerance : ± .002"
True Scale

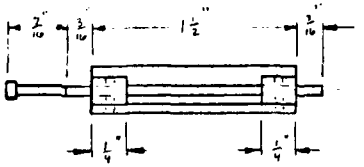

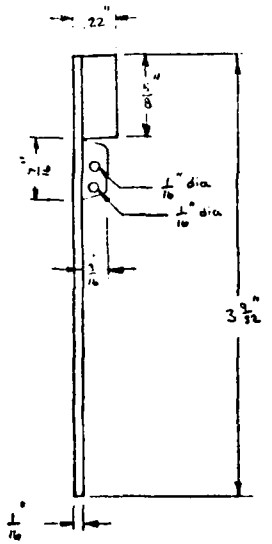

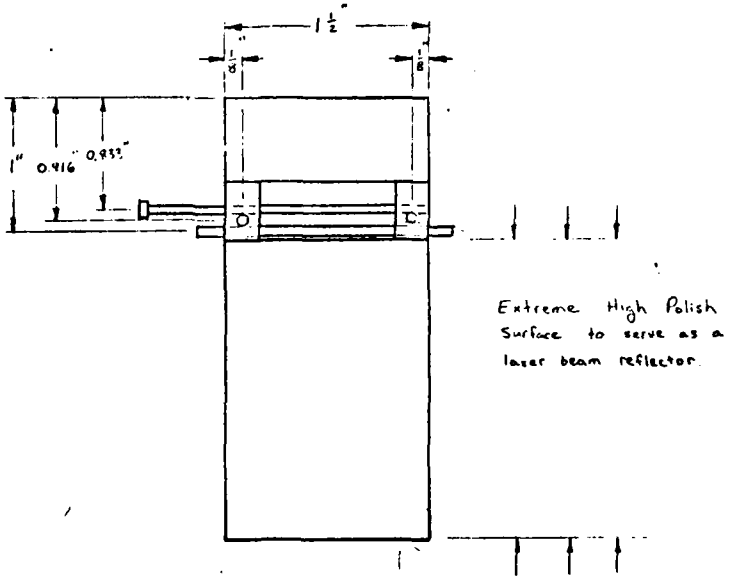

Extreme High Polish
Surface to serve as a
laser beam reflector.

Document does not
Reproduction

Laser Beam Switch Housing
Tilt Control

design: LT DJ PRASKA
AFIT/EN GEO-BID
Aug 81

True Scale
tolerance: ±.002"
material: aluminum

Note: There has been a slight change in the design of the Laser Beam Switch Housing floor as depicted.

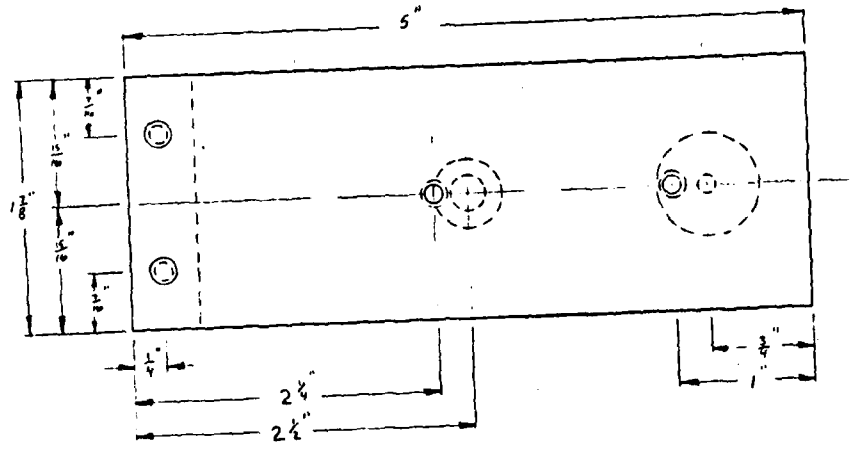

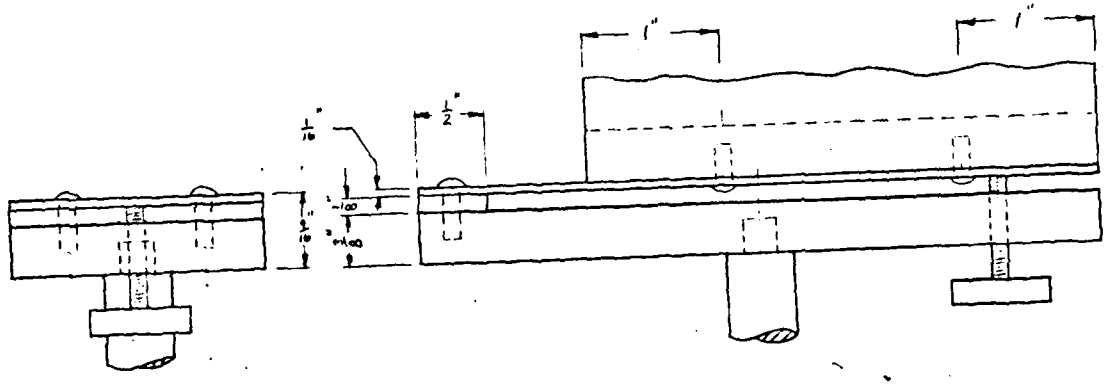

Reproduction does not

Articulated Arm
design: LT OJ Praska
AFIT/EN GEO-81D
Aug 81

Tolerance: ±.002"
Materials: Copper, Brass, Stainless Steel Tubing, and Aluminum

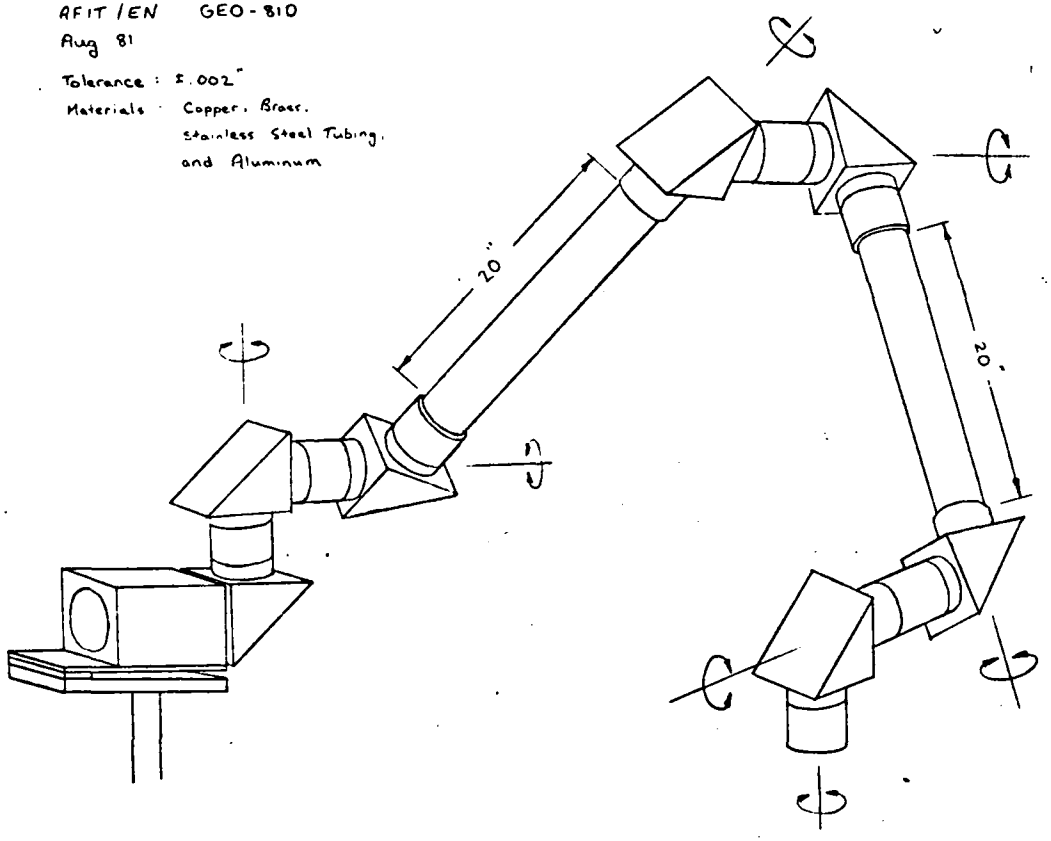

Permission for public reproduction not granted

Articulated Arm Optical Elbow with Swivel and without Mirror Plate

design: LT DJ PRASKA
AFIT/EN GED-81D
Aug 81

quantity: 7
tolerance: ± .002"
material: Brass and stainless steel Tubing

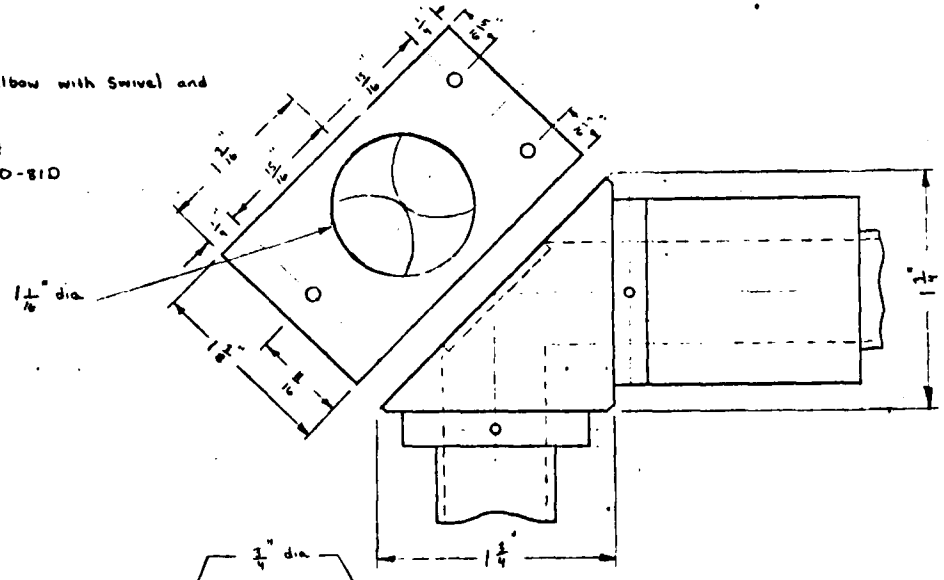

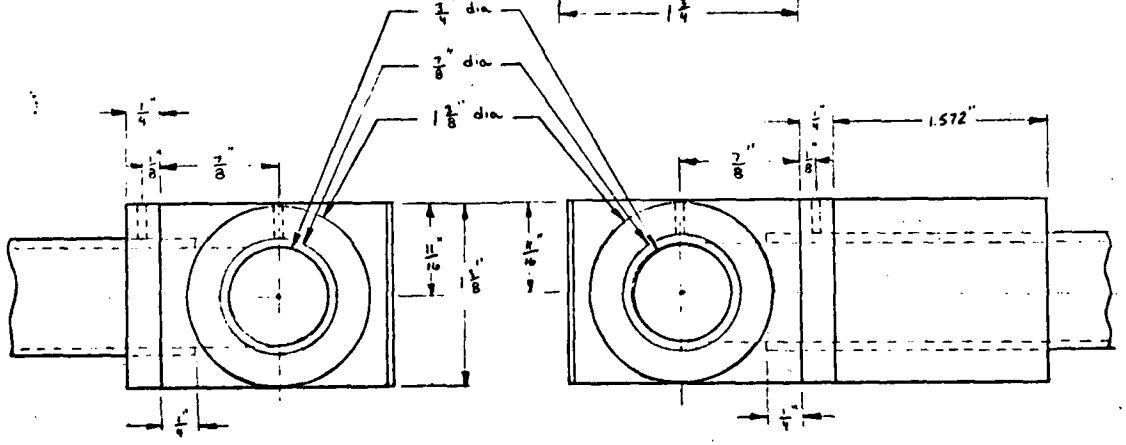

Document contains pages that may not reproduce legibly.

Cutaway View of Articulate Arm Optical Elbow with Swivel and Mirror Plate

design: LT DJ PRASKA
AFIT/EN
GEO-810 Aug 81

quantity: 7
tolerance: ±.002"
materials: Copper, Brass, and Stainless Steel Tubing

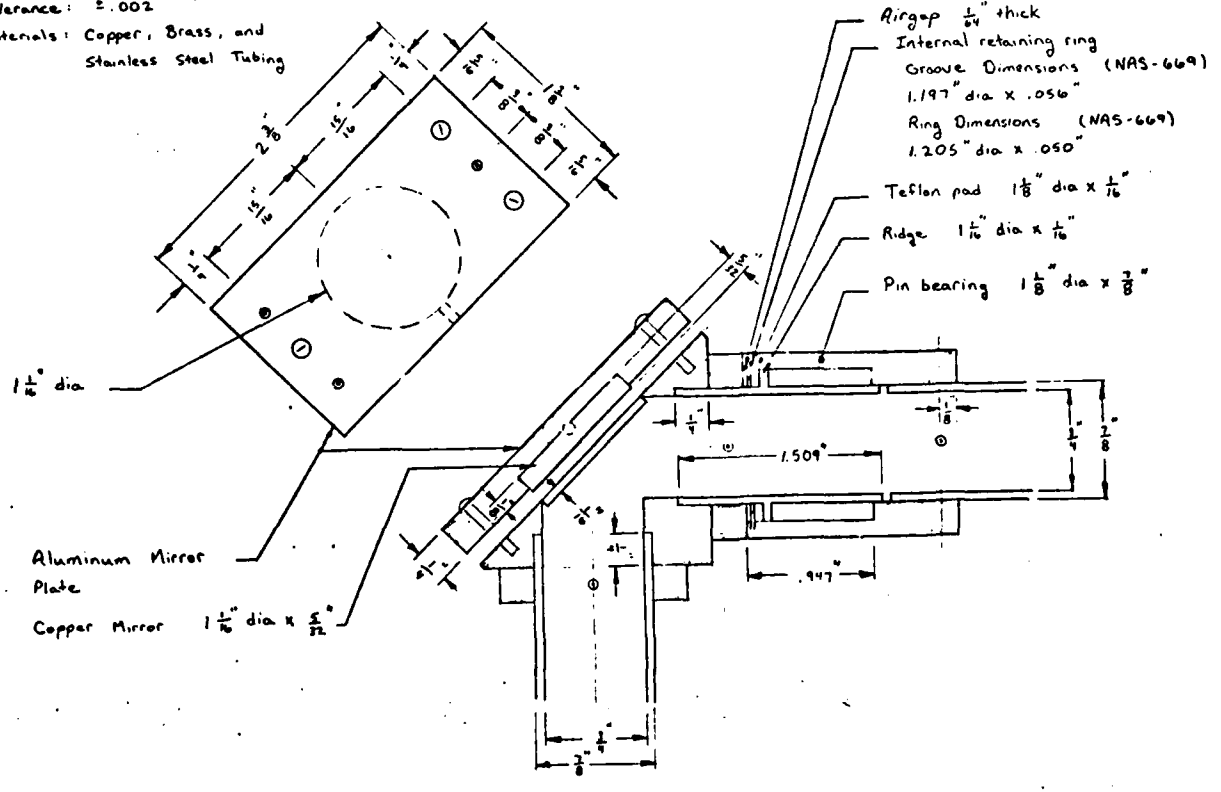

Reproduction not

Articulated Arm Base

design : LT OJ PRASKA
AFIT /EN
GEO-81D
Aug 81

material : aluminum
tolerance : ± .002"

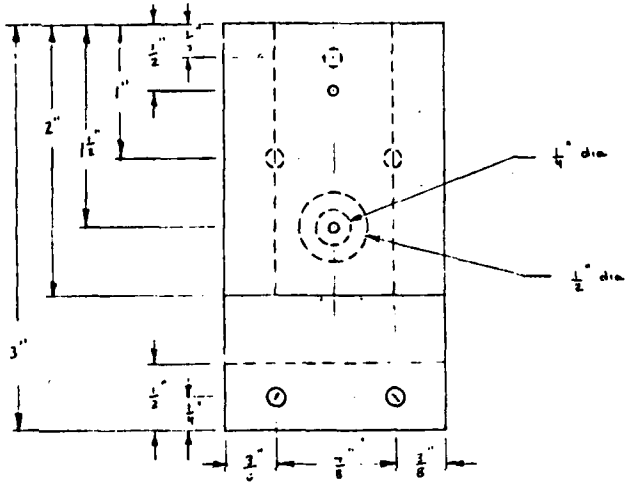

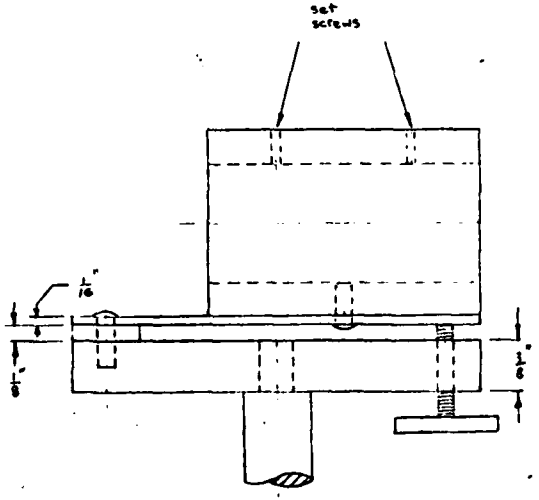

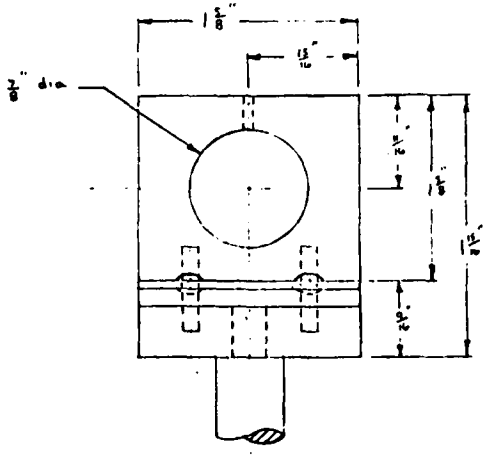

Copyright material does not permit [illegible] reproduction

Articulated Arm Base # 2

design: Capt DJ Praska
AFIT/EN
GEO-BID
Nov 81

material : aluminum

tolerance : ±.002"

quantity : 1 (one)

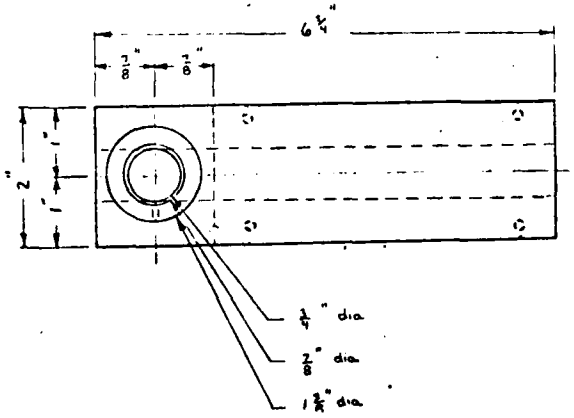

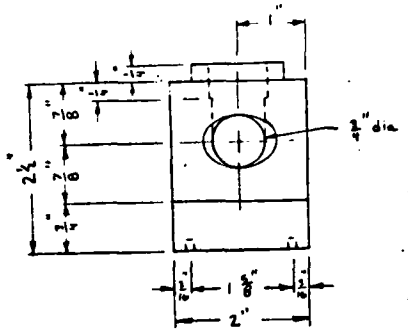

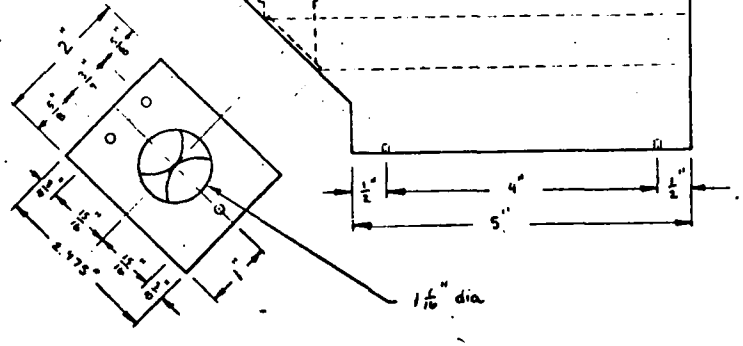

77

Reproduction

Articulated Arm Base Support
design: Capt DJ Praska
AFIT/EN GEO-81D
Nov 81
tolerance: ± .002"
material: aluminum
quantity: 2

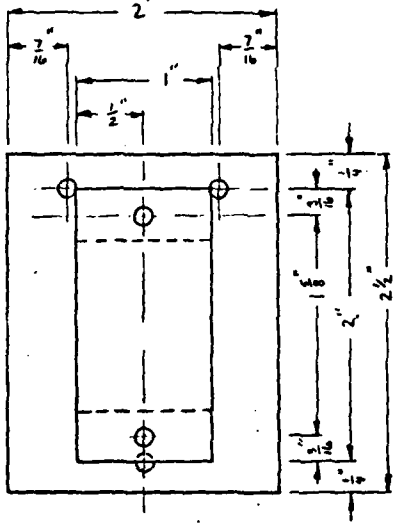

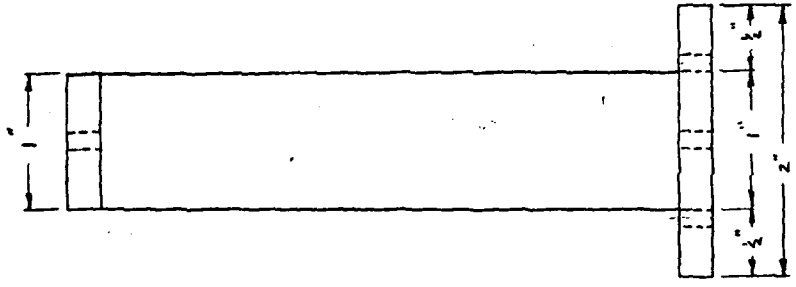

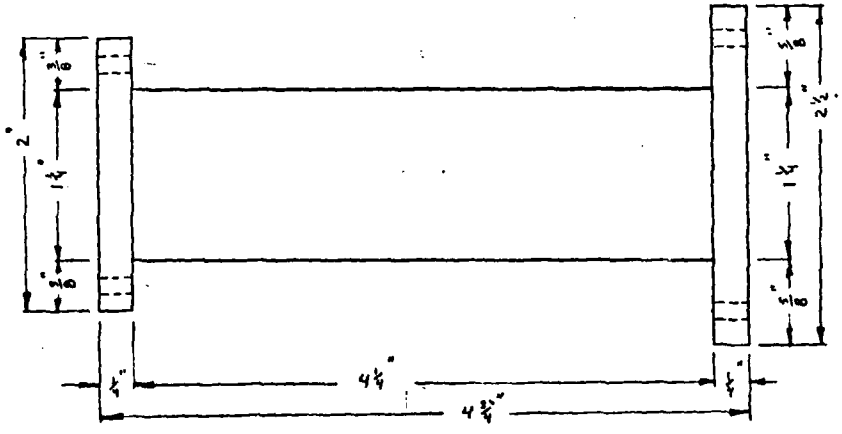

DTIC does not

Swivel Redesign for Articulated Arm

design: Capt D.J Praska
AFIT/EN GEO-810 Dec 81

quantity: 5
tolerance: ± 0.001" material: hardened aluminum Type 2024

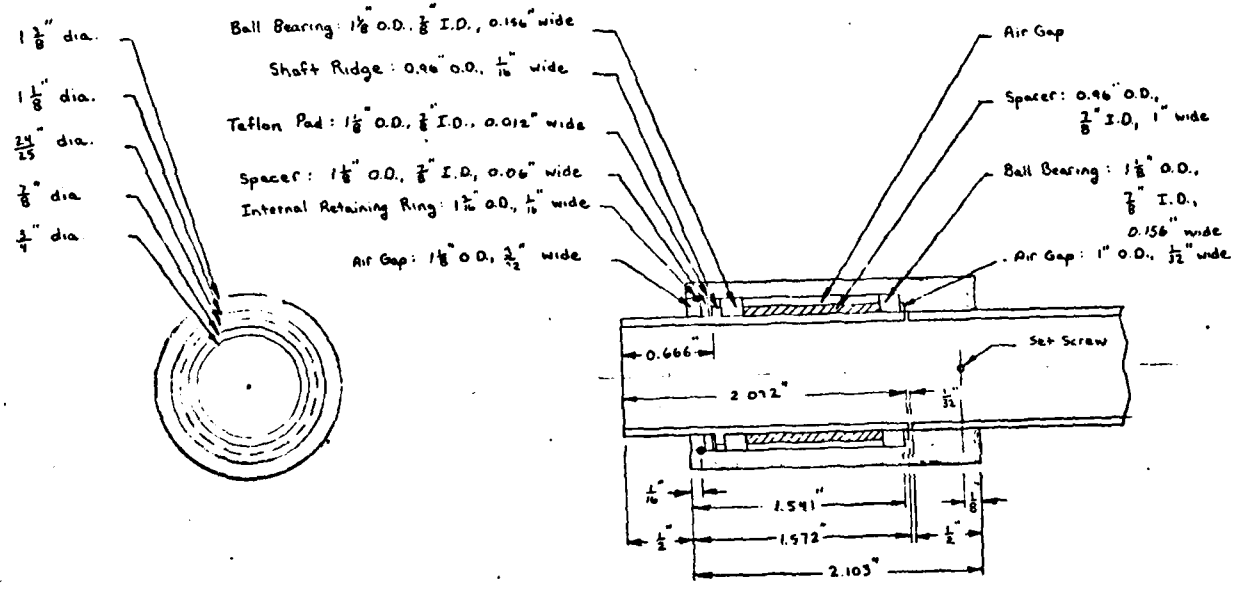

Capt [illegible] AFIT/EN
permission to quote or reproduction

Optical Elbow Mirror Plate for $\frac{1}{4}$" wide Mirror

design: Capt D.J. Praska
AFIT/EN GEO-81D Dec 81

quantity: 7
tolerance: ± 0.001"
material: hardened aluminum Type 2024

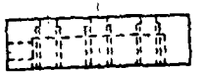

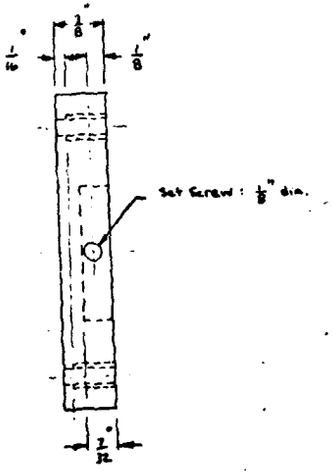

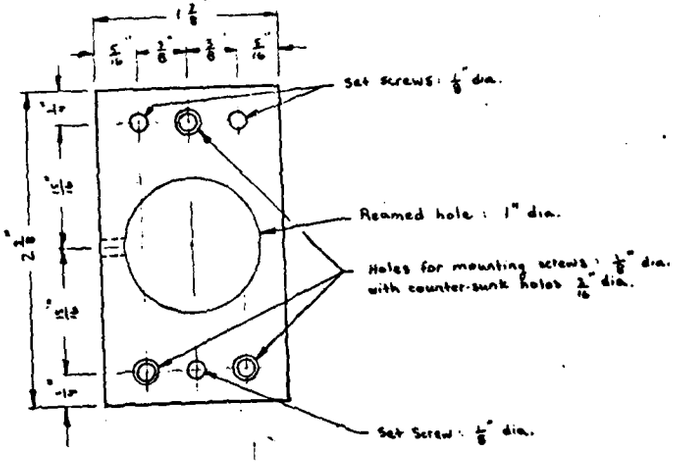

Reproduced at Government Expense

Optical Interface

design : LT DJ PRASKA
AFIT/EN GEO-81D
Aug 81

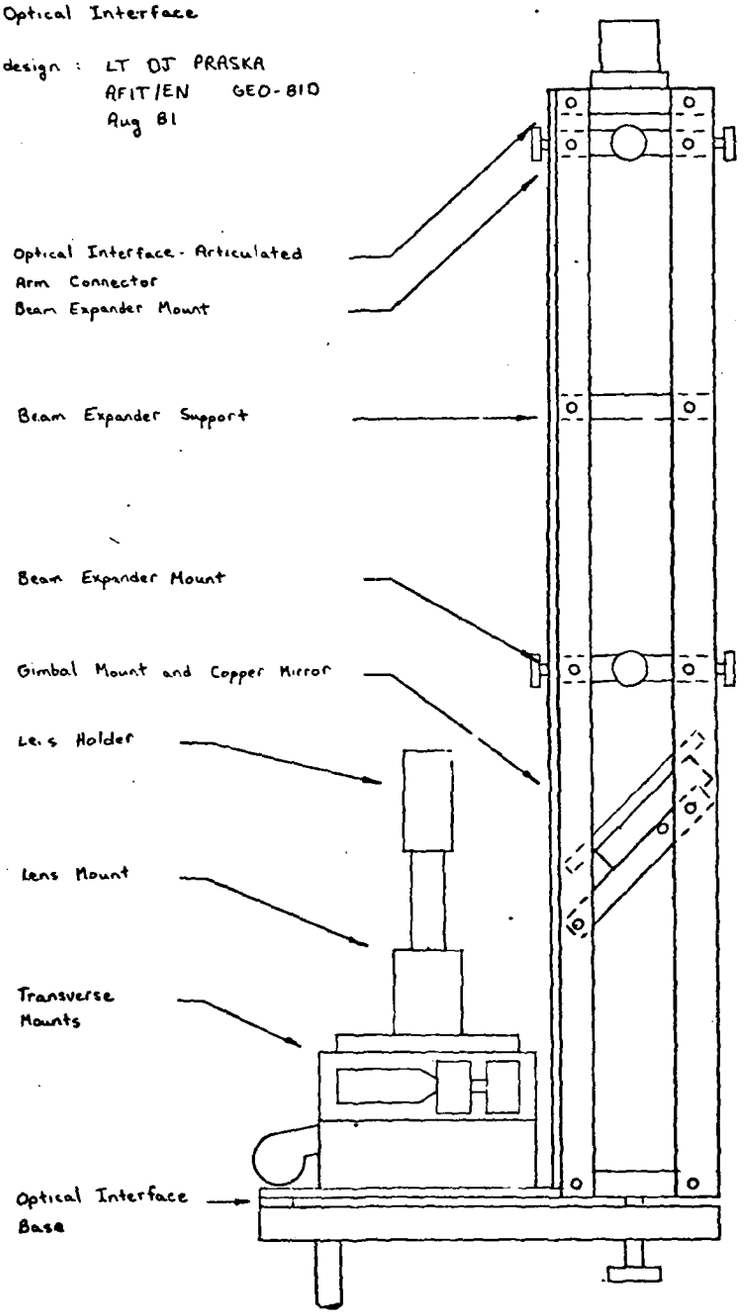

Optical Interface - Articulated Arm Connector

design: LT DJ PRASKA
AFIT/EN GEO-81D
Aug 81

material: aluminum and stainless steel tubing quantity: 1

tolerance: ±.002"

Note: Dimensions are essentially identical for the four sides of this component, in this view. All screw holes are threaded

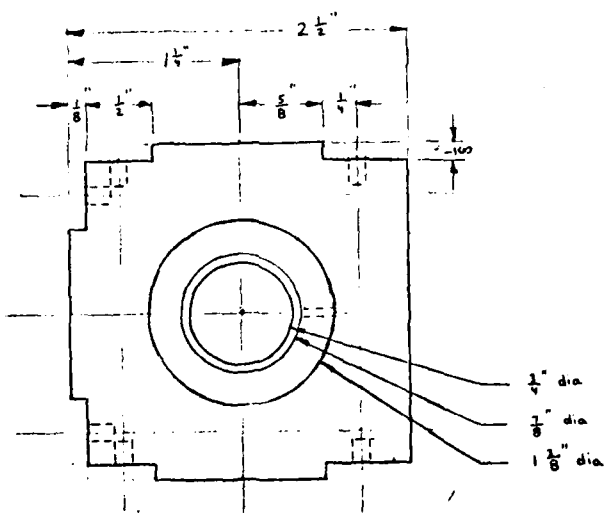

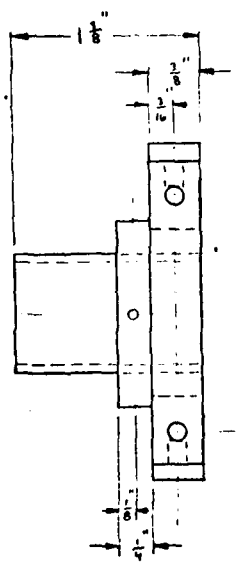

Copyright material reproduced with permission of the copyright owner. Further reproduction prohibited without permission. www.manaraa.com

Beam Expander Mounts

design: LT DJ PRASKA
AFIT/EN GEO-81D
Aug 81

material: aluminum quantity: 2

tolerance: ± .002"

Note: Dimensions are essentially identical for the four sides of this device in this view. All screw holes are threaded.

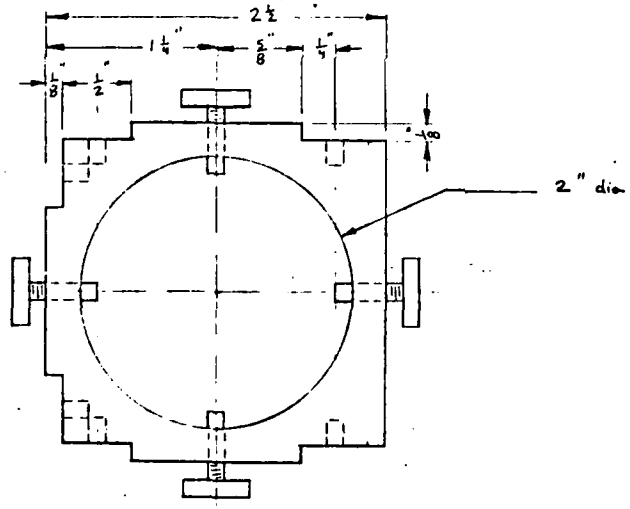

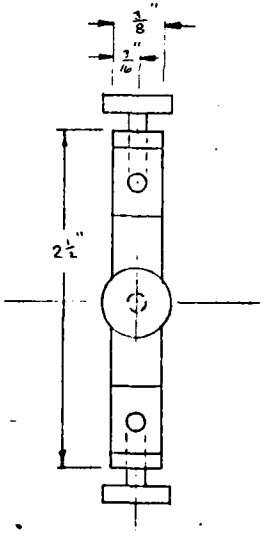

Beam Expander Support

design : LT DJ PRASKA
AFIT/EN GEO-81D
Aug 81

material : aluminum

tolerance : ± .002" quantity : 1

Note : Dimensions are essentially identical for three of the sides of this device shown in this view. All screw holes are threaded.

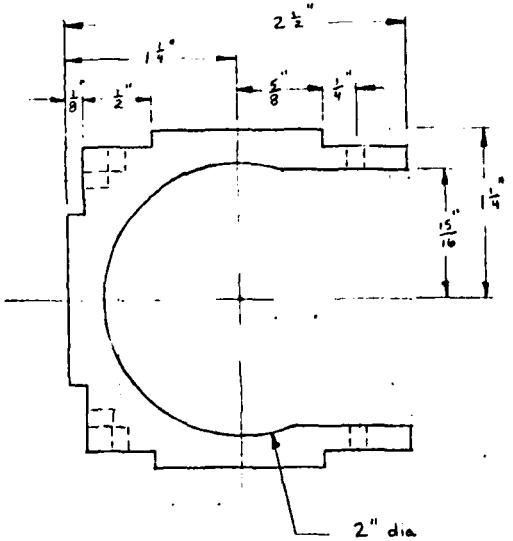

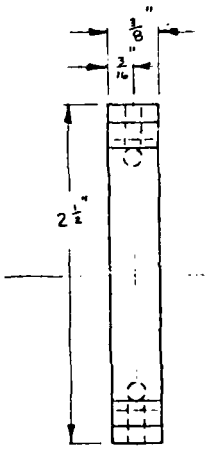

AD-A111 108 AIR FORCE INST OF TECH WRIGHT-PATTERSON AFB OH SCHOO--ETC F/G 6/18
DESIGN AND ADAPTATION OF AN OPTICAL SYSTEM FOR SLIT LAMP DELIVE--ETC(U)
DEC 81 D J PRASKA
UNCLASSIFIED AFIT/GEO/PH/81-6 NL

2 OF 2
AD
A111 108

END
DATE FILMED
3 82
DTIC

Gimbal Mount
design : LT DJ PRASKA
AFIT/EN GEO-81D
Aug 81
material : aluminum
tolerance : ±.002"

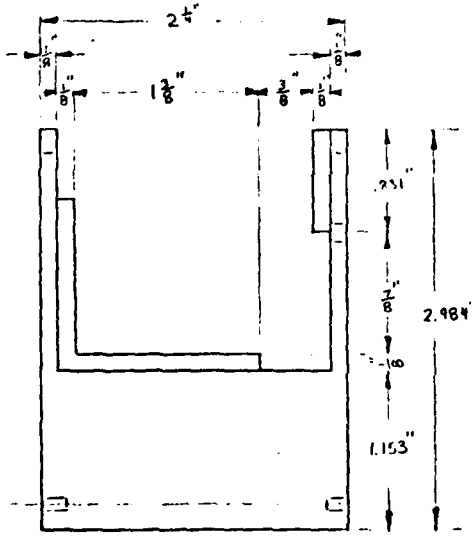

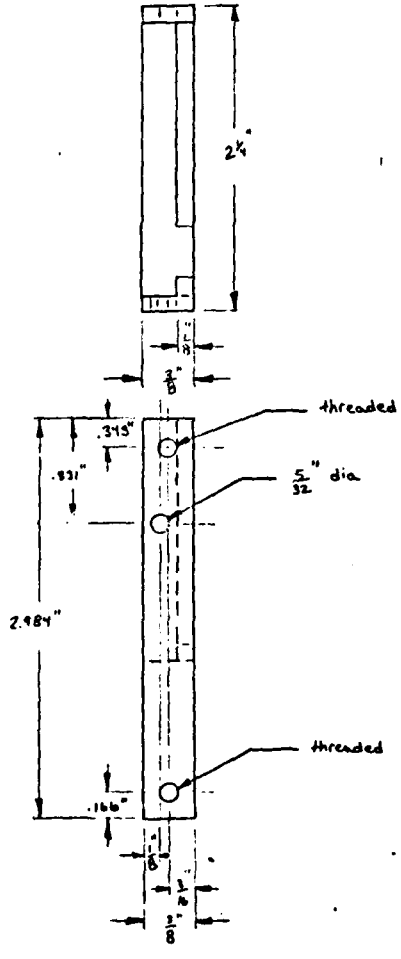

Copper Mirror

design : LT DJ PRASKA
AFIT/EN GEC-81D
Aug 81

material : copper

tolerance : ±.002"

Note : Back side must have an extremely high polish.

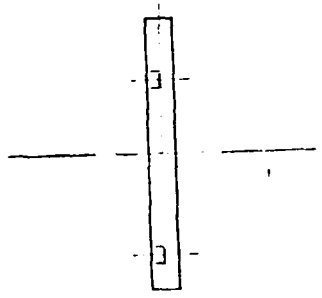

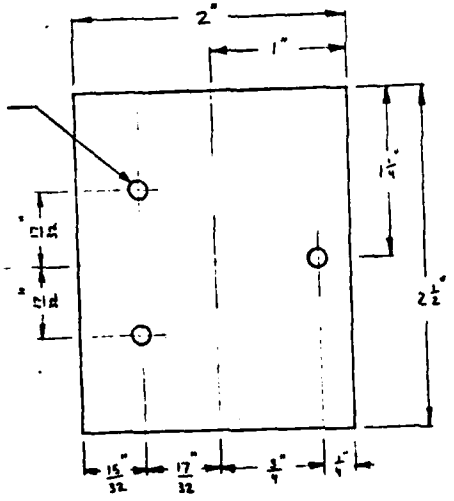

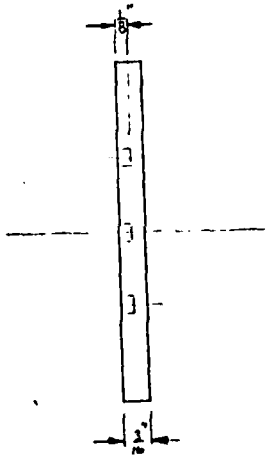

Portion may require reproduction

Meniscus Lens Mount

design : LT DJ PRASKA
AFIT/EN GEO-81D
Aug 81

material : aluminum

tolerance : ±.002" quantity : 1

Note: Dimensions are essentially identical for the four sides of this component shown in this view.

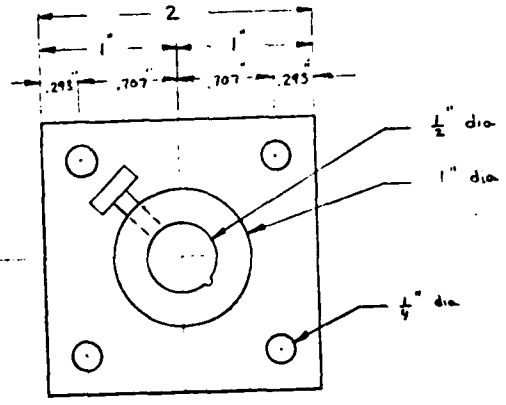

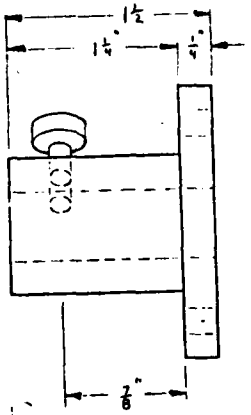

Copyright protection does not permit inclusion in electronic reproduction

Connecting Rods

design : LT DJ PRASKA
AFIT/EN GEO-81D
Aug 81

material : aluminum
tolerance : ±.002
Note : $\frac{1}{8}$" thickness for each rod

Set A , quantity : 2

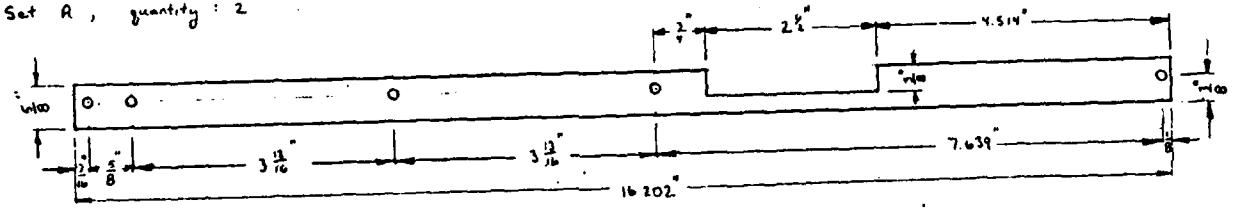

Set B . quantity : 2

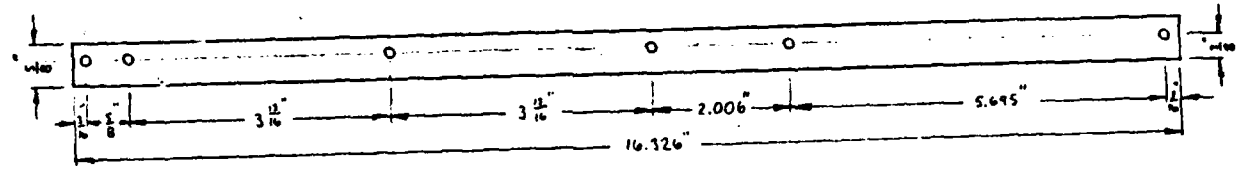

Set C , quantity : 2

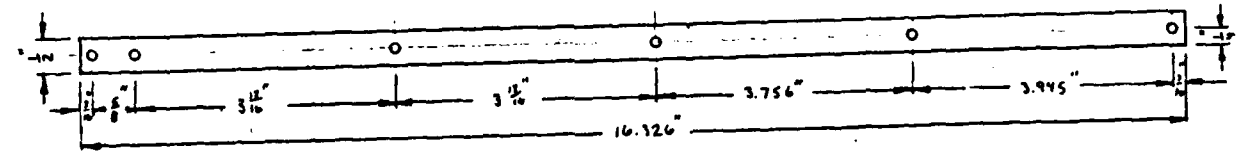

Copy available to DTIC does not permit fully legible reproduction

Optical Interface Base

design : LT DJ PRASKA
AFIT/EN GEO-81D
Aug 81

material : aluminum and stainless steel

tolerance : ± .002"

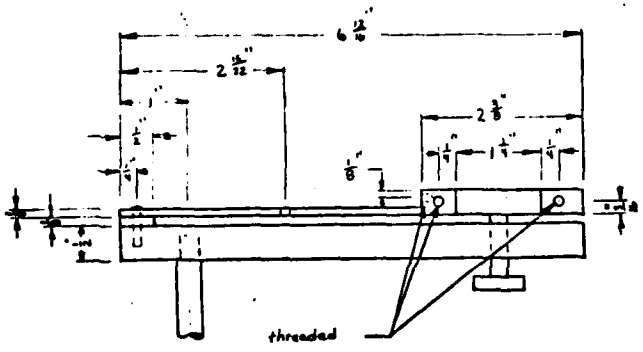

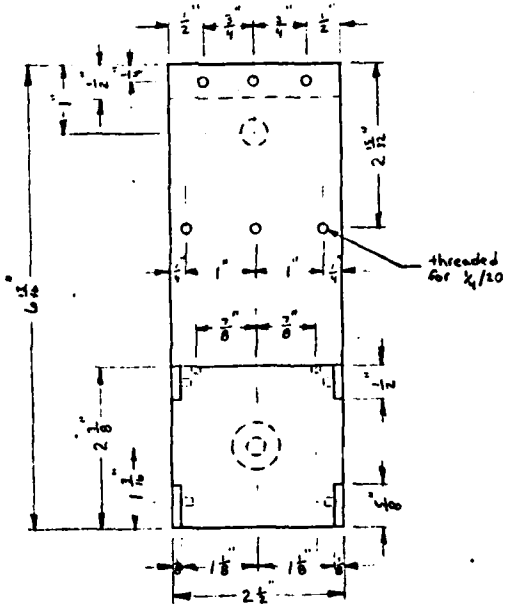

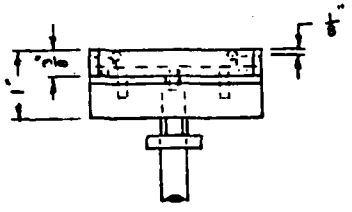

Vita

Douglas James Praska was born on 15 May 1954 in Oakes, North Dakota. He graduated from Oakes High School in 1972 and attended the University of North Dakota at Grand Forks shortly thereafter. He graduated from the university with a Bachelor of Science degree in Electrical Engineering, and a commission in the U.S. Air Force on 15 May 1977. He entered active duty in October of 1977, where he served as an electrical engineer within the Intelligence and Reconnaissance Division, Rome Air Development Center, Griffiss AFB, New York. In June of 1980, he entered the School of Engineering, Air Force Institute of Technology, Wright-Patterson AFB, Ohio. He is a member of the Institute of Electrical and Electronic Engineers.

Permanent Address: 418 South 5th Street
Oakes ND 58474

UNCLASSIFIED

SECURITY CLASSIFICATION OF THIS PAGE (When Data Entered)

REPORT DOCUMENTATION PAGE	READ INSTRUCTIONS BEFORE COMPLETING FORM
1. REPORT NUMBER: AFIT/GEO/PH/81-6	2. GOVT ACCESSION NO. AD-A111 125
3. RECIPIENT'S CATALOG NUMBER	
4. TITLE (and Subtitle): DESIGN AND ADAPTATION OF AN OPTICAL SYSTEM FOR SLIT LAMP DELIVERY OF A CO_2 LASER BEAM	5. TYPE OF REPORT & PERIOD COVERED: MS Thesis
	6. PERFORMING ORG. REPORT NUMBER
7. AUTHOR(s): DOUGLAS J. PRASKA, Capt USAF	8. CONTRACT OR GRANT NUMBER(s)
9. PERFORMING ORGANIZATION NAME AND ADDRESS: AF Institute of Technology (AFIT-EN), Wright-Patterson AFB OH 45433	10. PROGRAM ELEMENT, PROJECT, TASK AREA & WORK UNIT NUMBERS
11. CONTROLLING OFFICE NAME AND ADDRESS	12. REPORT DATE: December 1981
	13. NUMBER OF PAGES: 95
14. MONITORING AGENCY NAME & ADDRESS(if different from Controlling Office)	15. SECURITY CLASS. (of this report): UNCLASSIFIED
	15a. DECLASSIFICATION/DOWNGRADING SCHEDULE

16. DISTRIBUTION STATEMENT (of this Report)

Approved for Public Release; Distribution Unlimited.

17. DISTRIBUTION STATEMENT (of the abstract entered in Block 20, if different from Report)

[illegible] 19617.

18. SUPPLEMENTARY NOTES

28 JAN 1982

Fredric C. Lynch

FREDRIC C. LYNCH, Major, USAF
Director of Public Affairs

19. KEY WORDS (Continue on reverse side if necessary and identify by block number)

Radial Keratotomy
Corneal Scalpel
Articulated Arm
Ophthalmic Slit Lamp
CO_2 Laser

[illegible] of Technology (ATC)
[illegible] AFB, OH 45433

20. ABSTRACT (Continue on reverse side if necessary and identify by block number)

A Q-switched CO_2 laser was integrated to a standard ophthalmic slit lamp with the aid of an articulated arm. The laser-optical system, including the articulated arm, was adapted to a Nikon slit lamp to provide flexible control of high power 10.6 μm radiation for use in surgical cutting of the cornea. The articulated arm, consisting of seven optical elbows and seven copper mirrors, transmitted the CO_2 radiation from the laser to a 5X beam expander and a F/1 zinc selenide focusing lens attached to the slit lamp.

(Continued on Reverse)

DD FORM 1 JAN 73 1473 EDITION OF 1 NOV 65 IS OBSOLETE

UNCLASSIFIED

SECURITY CLASSIFICATION OF THIS PAGE (When Data Entered)

Block 20: ABSTRACT: (Cont'd)

Experimental results indicate that the integrated system can deliver 22 m spots of focused radiation on target with a corresponding Rayleigh range of approximately 36 μm. To demonstrate precise beam control, 9-0 Ethicon suture was ruptured with as little as 2.4 mJ of energy. Clear plastic sheets were cut to give an indication of what to expect in a corneal incision. Finally, hog corneas were incised by an ophthalmologist.

The experimental work was complemented by a parametric study relating focused spot diameter, Rayleigh range, and laser wavelength for a series of wavelengths extending from 0.249 to 10.6 μm. The results of the parametric plots may be used as an aid when selecting optimal laser parameters for given applications in ocular surgery.

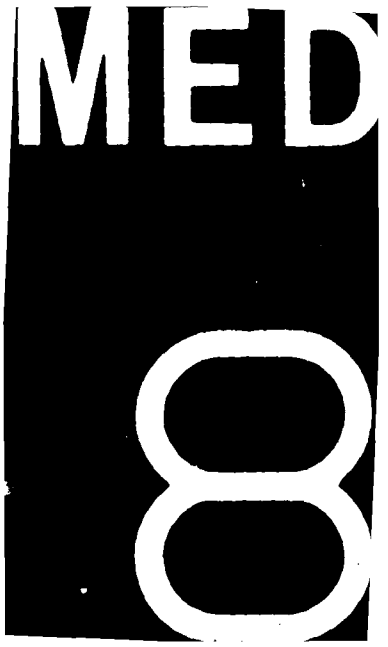
MED
8